

SoK: Comparing Different Membership Inference Attacks with a Comprehensive Benchmark

Jun Niu*, Xiaoyan Zhu*, Moxuan Zeng†, Ge Zhang*, Qingyang Zhao*, Chunhui Huang†, Yangming Zhang†, Suyu An†, Yangzhong Wang†, Xinghui Yue‡, Zhipeng He§, Weihao Guo†, Kuo Shen*, Peng Liu¶, Yulong Shen*, Xiaohong Jiang||, Jianfeng Ma*, Yuqing Zhang***

*Xidian University, {niu jun, 21151213588}@stu.xidian.edu.cn

, {xyzhu, ylshen, jfma}@mail.xidian.edu.cn, zhangg@nipc.org.cn, shenkuo_xdu@163.com

†Hainan University, zengmoxuan@hainanu.edu.cn, {huangch, zhangym, an sy, wangyz21, guowh}@nipc.org.cn

‡Yanshan University, yxh0314@stumail.ysu.edu.cn

§Xi'an University of Posts & Telecommunications, hezhp@nipc.org.cn

¶Pennsylvania State University, pliu@ist.psu.edu

||Future University of Hakodate, jiang@fun.ac.jp

***University of Chinese Academy of Sciences, zhanyq@ucas.ac.cn

Abstract—Membership inference (MI) attacks threaten user privacy through determining if a given data example has been used to train a target model. However, it has been increasingly recognized that the “comparing different MI attacks” methodology used in the existing works has serious limitations. Due to these limitations, we found (through the experiments in this work) that some comparison results reported in the literature are quite misleading. In this paper, we seek to develop a comprehensive benchmark for comparing different MI attacks, called MIBench, which consists not only the evaluation metrics, but also the evaluation scenarios. And we design the evaluation scenarios from four perspectives: the distance distribution of data samples in the target dataset, the distance between data samples of the target dataset, the differential distance between two datasets (i.e., the target dataset and a generated dataset with only nonmembers), and the ratio of the samples that are made no inferences by an MI attack. The evaluation metrics consist of ten typical evaluation metrics. We have identified three principles for the proposed “comparing different MI attacks” methodology, and we have designed and implemented the MIBench benchmark with 84 evaluation scenarios for each dataset. In total, we have used our benchmark to fairly and systematically compare 15 state-of-the-art MI attack algorithms across 588 evaluation scenarios, and these evaluation scenarios cover 7 widely used datasets and 7 representative types of models. All codes and evaluations of MIBench are publicly available at <https://github.com/MIBench/MIBench.github.io/blob/main/README.md>.

1. Introduction

Recently, machine learning (ML), especially deep learning (DL), has achieved tremendous progress in various domains such as image recognition [1], speech recognition [2],

* Xiaoyan Zhu and Yuqing Zhang are the corresponding authors.

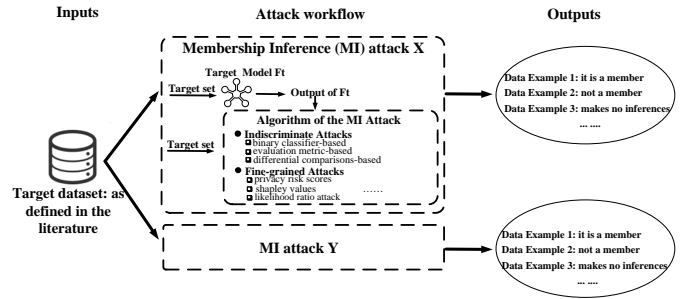


Figure 1. A summary of MI attack workflows.

natural language processing [3] and medical analysis [4]. However, many researches have demonstrated that ML models are vulnerable to various attacks, such as property inference attacks [5], adversarial attacks [6], model poisoning attacks [7] and membership inference attacks [8], [9], [10], [11].

Among these attacks, Membership Inference (MI) attacks [8], [9], [12], [13], [14] determine whether a data example is inside the training dataset of the target model or not. The workflows of the existing MI attacks are summarized in Figure 1: although all the existing MI attack algorithms have the same inputs, indiscriminate attack algorithms (e.g., [8], [9], [10], [12], [13], [14], [15], [16], [17], [18], [19], [20], [21], [22], [23], [24], [25], [26], [27], [28], [29], [30], [31], [32], [33], [34], [35], [36], [37], [38], [39], [40], [41], [42], [43], [44], [45], [46], [47], [48], [49]) and fine-grained attack algorithms (e.g., [50], [51], [52], [53], [54], [55], [56]) could have different (kinds of) outputs. In particular, every attack algorithm has two inputs: (1) the **target dataset**, which holds the set of given to-be-inferred data examples; (2) the outputs of the **target model** against each given data example. For indiscriminate attack algo-

gorithms, their output is binary, telling whether a given data example is a member or not. In contrast, fine-grained attack algorithms firstly make (fine-grained) Yes/No decisions on making an inference or not. When a No decision is made on data example x , the output will be “no inference is made on x ” (e.g., Data Example 3 showed in Figure 1).

Due to the importance of MI attacks, researchers have proposed many MI attacks in recent years. However, it has been increasingly recognized that the “comparing different MI attacks” methodology used in the existing works has serious limitations. Due to these limitations, we found (through the experiments in this work) that some comparison results reported in the literature are quite misleading.

To illustrate the serious limitations, let’s summarize the main factors determining when an MI attack is more effective and when it is less effective. First of all, two primary factors have been recognized in all the existing works: the kind of data in the target dataset; and the type of the target model. In order to incorporate these two factors in evaluating attack effectiveness, all the existing works use multiple target datasets and multiple types (e.g., MLP, ResNet, DenseNet) of target models. Second, based on the experiment results which we will shortly present in Section 6, we found the following factors. **Factor 1.** It is found in our experiments (see Section 6.1) that the effectiveness of an MI attack could be highly sensitive to the distance distribution of data samples in the target dataset. **Factor 2.** It is found in our experiments, which we will shortly present in Section 6.2, that the effectiveness of an MI attack could be highly sensitive to the distances between data samples of the target dataset. The larger the distance between data samples of the target dataset, the higher the attacker’s **membership advantage (MA)**. By “membership advantage”, we mean the difference between an MI attack’s true and false positive rates (e.g., $MA = TPR - FPR$ [13]). In addition, we found that the existing state-of-the-art MI attacks can achieve high inference accuracy and low FPR (false positive rate) simultaneously when the distances between data samples of the target dataset are carefully controlled. **Factor 3.** It is found in our experiments (see Section 6.3) that the effectiveness of an MI attack could be very sensitive to the differential distance (i.e., Maximum Mean Discrepancy (MMD) [57]) before and after a data example is moved from the target dataset to a generated dataset with only nonmembers. In addition, we found that in general Factor 3 has greater influence (on attack effectiveness) than Factor 2. **Factor 4.** Since fine-grained attack algorithms make no inferences on certain data examples, it seems *unfair* to use the same number of data examples when comparing indiscriminate attack algorithms and fine-grained attack algorithms.

These four factors clearly indicate that a “comparing different MI attacks” methodology will not be convincing unless the following requirements are met. **(R1)** A set of target datasets following different representative distance distributions should be used when comparing different MI attacks. Attack A could be more effective than Attack B when the target dataset follows one distribution but less effective under another distribution. **(R2)** A set of target

datasets having different distances between data samples should be used when comparing different MI attacks. **(R3)** A set of target datasets having different differential distances should be used when comparing different MI attacks. **(R4)** When comparing an indiscriminate attack algorithm and a fine-grained attack algorithm, the target datasets used for evaluating the first algorithm should hold a smaller number of data examples.

The last 4 columns in Table 1 summarize whether these four requirements are satisfied in thirteen most representative existing works on MI attacks. Unfortunately, we find that (a) 8 out of the 15 existing works fail to meet any of the four requirements; (b) 7 out of the 15 existing works only manage to meet one of the four requirements. In particular, none of the 15 existing works meets requirement R1; none of the 15 existing works meets requirement R2; 12 out of the 15 existing works don’t meet requirement R3.

In this work, we seek to develop a comprehensive benchmark for comparing different MI attacks. The primary design goal of our benchmark, called **MIBench**, is to meet *all* of these 4 requirements. In order to achieve this goal, our key insights are as follows. **Insight A.** Although it is widely recognized in the existing works that evaluation metrics (e.g., the “membership advantage” metric) play an essential role in comparing different MI attacks, we find that even if the employed metrics are appropriate, the comparison results can still suffer from *poor explanations*. For example, researchers have already noticed the following: (a1) one MI attack algorithm could suffer from fairly different evaluation results (i.e., metric measurements) against different target datasets: it is usually difficult to explain the lack of coherence cross datasets. (a2) MI attack A is more effective than attack B against target dataset D1, but attack B is more effective than attack A against target dataset D2. In such situations, it is usually very *difficult to draw general conclusions* on when attack A would be more effective and when attack B would be more effective. (a3) Many MI attacks suffer from low precision against widely-used test datasets. For example, BlindMI-Diff [14] suffers from a precision of 50.01%. However, it is usually difficult to explain why higher precision is not achieved. **Insight B.** We find that the above-mentioned four factors can be used to significantly improve the **explainability** of a “comparing different MI attacks” methodology. For example, the four factors in many cases enable one to draw such general conclusions as “attack A is more effective than attack B when the following two conditions are simultaneously met: (c1) the distance distribution of data samples in a target dataset follows normal distribution; (c2) the distances between data samples of the target dataset are 6.000.”

Based on these insights, our benchmark consists not only the evaluation metrics, but also the evaluation scenarios. Based on the above-mentioned four factors, we design the evaluation scenarios from **four perspectives**: the distance distribution of data samples in the target dataset, the distance between data samples of the target dataset, the differential distance between two datasets (i.e., the target dataset and a generated dataset with only nonmembers), and the ratio of

the samples that are made no inferences by an MI attack. Moreover, each perspective corresponds to a control variable and so there are in total four **control variables** in our evaluation scenarios. The evaluation metrics consist of ten evaluation metrics (i.e., accuracy, FPR, TPR, precision, f1-score, FNR, MA, AUC, TPR @ fixed (low) FPR, Threshold at maximum MA): they are widely used in the existing works on MI attacks (see Section 5.2.2).

Contributions. The main contribution of this work are as follows. First, we have identified three principles for the proposed “comparing different MI attacks” methodology. Second, following these principles, we have designed and implemented the MIBench benchmark with 84 evaluation scenarios for each dataset. For each evaluation scenario, we have designed the particular values of the four above-mentioned control variables; and we have created the corresponding target datasets through customizing seven widely-used datasets in the research area of MI attacks. (It should be noticed that all the evaluation scenarios use the same set of evaluation metrics.) Third, we have used our benchmark to systematically compare 15 state-of-the-art MI attack algorithms. For this purpose, we have downloaded the code of the following 15 MI attacks from GitHub: NN_attack [8], Loss-Threshold [13], Label-only [13], Top3-NN attack [9], Top1-Threshold [9], BlindMI-Diff-w [14], BlindMI-Diff-w/o [14], BlindMI-1CLASS [14], Top2+True [14], Privacy Risk Scores [52], Shapley Values [54], Positive Predictive Value [50], Calibrated Score [56], Distillation-based [53], Likelihood ratio attack [55]. And we have conducted comparative evaluations of the 15 MI attacks using the above-mentioned evaluation scenarios. In total, we used 588 evaluation scenarios to fairly and systematically compare the existing MI attacks. These evaluation scenarios cover 7 datasets, which are widely used in the existing works on MI attacks, and 7 representative types of models.

2. Background

2.1. Membership Inference Attacks

A target ML model \mathbb{F}_T is described as a ML model trained on a certain target training dataset \mathcal{D}_{train} . And the MI attacks aim to determine whether a data point x is in the target training dataset \mathcal{D}_{train} . More generally, given a data point x_T , extra knowledge of the adversary \mathcal{K} , a targeted machine learning model \mathbb{F}_T , and the workflow of an MI attack (called the attack model \mathbb{AM}) is defined as the following. $\mathbb{AM} : \{\mathbb{F}_T(x_T), \mathcal{K}\} \Rightarrow \{0, 1\}$, here the MI attack model \mathbb{AM} is a binary classifier and 1 means the target data point x_T is a member of the \mathcal{D}_{train} and 0 is a non-member (inside “T” means a target model or data point).

2.2. Threat Model

Black-box attack. The attackers only know the outputs of the target model (e.g., confidence score vectors) and mainly utilize them for training a binary classifier to determine

the membership of a data sample. **Gray-box attack.** The attackers not only control the certain target models’ inputs and outputs, but know the distributions of training data trained the target model. **White-box attack.** The attackers know all information of the target model and training data.

3. Motivation and Overview

3.1. Motivation

The proposed benchmark is motivated by the following observations. **Observation 1.** We find that even if the employed metrics are appropriate, the comparison results can still suffer from poor explanations. For example, researchers have already noticed the following: (a1) One MI attack algorithm could suffer from fairly different evaluation results (i.e., metric measurements) against different target datasets: it is usually difficult to explain the lack of coherence cross datasets. In many cases, although the different target datasets have different data semantics (e.g., CIFAR100 holds 100 kind of data, while CH-MNIST holds 8 kind of data), strong correlation between the data semantics and the evaluation results is hard to identify. (a2) MI attack A is more effective than attack B against target dataset D1, but attack B is more effective than attack A against target dataset D2. In such situations, it is usually very difficult to draw general conclusions on when attack A would be more effective and when attack B would be more effective. For example, the NN_attack [8] (e.g., MA=34.51%) is more effective than Label-only [13] attack (e.g., MA=32.77%) against CIFAR10, but the Label-only [13] attack (e.g., MA=70.6%) is more effective than NN_attack [8] (e.g., MA=58.54%) against CIFAR100. (a3) Many MI attacks suffer from low precision (e.g., NN_attack [8] (51.7%), Label-only [13] (50.5%) and BlindMI-Diff [14] (50.01%)) against widely-used test datasets. However, it is usually difficult to explain why higher precision is not achieved.

Observation 2. We find that although all the existing works pay adequate attention to two primary factors determining when an MI attack is more effective, i.e., the semantics of data examples in the target dataset and the type of the target model, the existing works pay inadequate attention to three additional main factors. (Factor 1) We find that the effectiveness of an MI attack could be highly sensitive to the distance distribution of data samples in the target dataset. (Factor 2) We find that the effectiveness of an MI attack could be highly sensitive to the distance between data samples of the target dataset. (Factor 3) We find that the effectiveness of an MI attack could be very sensitive to the differential distance (i.e., MMD [57]) before and after a data example is moved from the target dataset to a generated dataset with only nonmembers. For example, (b1) without incorporating Factor 1, the comparison evaluation results in [8], [9], [13], [14], [50], [52], [53], [54], [55], [56] are difficult to provide insightful explanations on low precision (e.g., NN_attack [8] (51.7%), Label-only [13] (50.5%) and BlindMI-Diff [14] (50.01%)) or high FPR [8], [49]. (b2) Without incorporating Factor 2, the comparison

TABLE 1. CATEGORIZATIONS OF 15 MEMBERSHIP INFERENCE ATTACK ALGORITHMS IN MIBENCH, ACCORDING TO TEN PERSPECTIVES, INCLUDING *treat models, shadow model, attack model, extra data, ground-truth, the number of inferring, evaluation metrics, inputs, outputs* AND *different kinds of evaluation requirements*.

Attack Algorithm	Threat Model			Shadow Model	Attack Model	Extra Data	Ground Truth	# Inference	Evaluation Metrics	Inputs	Outputs	Evaluation Requirements (ERs)			
	blk.	gry.	whi.									DisDistri.	DataSampleDist.	DifferDist.	RatNoInf.
NN_attack [8]	✓	✗	✗	m	m	✗	✓	w	1+2	\mathcal{D}_t	1	✗	✗	✗	✗
Loss-Threshold [13]	✓	✗	✗	1	✗	✗	✓	w	1+2+7	\mathcal{D}_t	1	✗	✗	✗	✗
Label-only [13]	✓	✗	✗	✗	✗	✗	✓	w	1+2+7	\mathcal{D}_t	1	✗	✗	✗	✗
Top3-NN attack [9]	✓	✗	✗	1	1	✗	✓	w	1+2	\mathcal{D}_t	1	✗	✗	✗	✗
Top1-Threshold [9]	✓	✗	✗	✗	✗	✓	✓	w	1+2+8	\mathcal{D}_t	1	✗	✗	✗	✗
BlindMI-Diff-w [14]	✓	✓	✓	✗	✗	✓	✓	w	1+2+3	\mathcal{D}_t	1	✗	✗	✓	✗
BlindMI-Diff-w/o [14]	✓	✓	✓	✗	✗	✓	✓	w	1+2+3	\mathcal{D}_t	1	✗	✗	✓	✗
BlindMI-ICLASS [14]	✓	✓	✓	✗	✗	✓	✓	w	1+2+3	\mathcal{D}_t	1	✗	✗	✓	✗
Top2+True [14]	✓	✗	✗	m	m	✗	✓	w	1+2+3	\mathcal{D}_t	1	✗	✗	✗	✗
Privacy Risk Scores [52]	✓	✗	✗	m	✗	✗	✓	p	1+2+4	\mathcal{D}_t	1+2	✗	✗	✗	✓
Shapley Values [54]	✓	✗	✗	m	✗	✗	✓	p	1+2+4+5	\mathcal{D}_t	1+2	✗	✗	✗	✓
Positive Predictive Value [50]	✓	✗	✗	m	✗	✗	✓	p	1+2+6+7+9	\mathcal{D}_t	1+2	✗	✗	✗	✓
Calibrated Score [56]	✓	✗	✗	m	✗	✗	✓	w	1+2+4+8+9	\mathcal{D}_t	1	✗	✗	✗	✗
Distillation-based Thre. [53]	✓	✗	✗	m	✗	✗	✓	w	1+2+8+9	\mathcal{D}_t	1	✗	✗	✗	✗
Likelihood ratio attack [55]	✓	✗	✗	m	✗	✗	✓	w	8+9+10	\mathcal{D}_t	1	✗	✗	✗	✓

- a) **Threat Model:** blk. → Black-box; gry. → Gray-box; whi. → White-box;
b) **# Inference:** w → the whole data in the target dataset; p → the part of data in the target dataset;
c) **Shadow Model:** 1 → one shadow model; m → multiple shadow models;
d) **Attack Model:** 1 → one attack model; m → multiple attack models;
e) **Evaluation Metrics:** 1 → **precision**, namely the ratio of true positives to the sum of true positive and false positives;
2 → **recall**, namely the ratio of true positives to the sum of true positives and false negatives;
3 → **f1-score**, namely the harmonic mean of precision and recall;
4 → **accuracy**, namely the percentage of data records with correct membership predictions by the attack model;
5 → **average membership privacy risk score**, namely the average over the membership privacy risk scores assigned to training data records;
6 → **positive predictive value (PPV)**, namely the ratio of true members predicted among all the positive membership predictions;
7 → **membership advantage (MA)**, namely the difference between the true positive rate and the false positive rate (e.g., MA = TPR - FPR);
8 → **the area under ROC curve (AUC)**, namely the area under the Receiver Operating Characteristic (ROC) curve;
9 → **false positive rate (FPR)**, namely the ratio of nonmember samples are erroneously predicted as members;
10 → **a TPR at low FPR**, namely the true-positive rate at low (e.g., $\leq 0.1\%$) false-positive rates;
f) **Outputs:** 1 → predict the target data is (or is not) a member; 2 → make no inferences about the target data;
g) **Evaluation Requirements:** DisDistri. → the distance distribution of data samples in the target dataset; DataSampleDist. → distance between data samples of the target dataset; DifferDist. → the differential distance before and after moving a data sample; RatNoInf. → the ratio of the samples that are made no inferences by an MI attack;
h) \mathcal{D}_t : means a target data or dataset; “✓”: means the adversary needs (considers) the knowledge (ER); “✗”: indicates the knowledge (ER) is not necessary (be considered).

evaluation results in [8], [9], [13], [14], [50], [52], [53], [54], [55], [56] are difficult to explain why the higher precision is not achieved. (b3) Without incorporating Factor 3, the comparasion evaluation results in [8], [9], [13], [50], [52], [53], [54], [55], [56] are difficult to explain why the low FPR and higher accuracy are not achieved simultaneously.

Based on above key observations, we are strongly motivated to incorporate the above-mentioned factors into a new benchmark and use the benchmark to fairly and systematically compare different MI attacks. In addition, we are strongly motivated to develop a new “comparing different MI attacks” methodology which has **significantly improved ability to explain** the comparative evaluation results.

3.2. Overview

To alleviate the dilemma of the existing MI attacks, in this work, we seek to develop a comprehensive benchmark for comparing different MI attacks. The primary design goal of our benchmark, called **MIBench** (Section 5), is to meet *all* of above-mentioned 4 requirements (see Section 1). Our benchmark consists not only the evaluation metrics (Section 5.2.2), but also the evaluation scenarios (Section 5.2.1). Based on the above-mentioned four factors (see Section 1), we design the evaluation scenarios from **four perspectives**: the distance distribution of data samples in the target dataset,

the distance between data samples of the target dataset, the differential distance between two datasets (i.e., the target dataset and a generated dataset with only nonmembers), and the ratio of the samples that are made no inferences by an MI attack. Moreover, each perspective corresponds to a control variable and so there are in total four **control variables** in our evaluation scenarios. The evaluation metrics consist of ten widely used evaluation metrics (i.e., accuracy, FPR, TPR, precision, f1-score, FNR, MA, AUC [55], TPR @ fixed (low) FPR [55], Threshold at maximum MA) (see Section 5.2.2).

Based on the evaluation framework (Section 5), we also present how to use the evaluation framework (Section 6) to fairly and effectively evaluate the real performance of an MI attack. There are four steps before using the evaluation framework. **Step 1: Construct the distance distribution of data samples in the target dataset (CV1) (Section 6.1).** For a target dataset, we first input all data samples (e.g., n) in the target dataset to the target model and get the corresponding output probabilities, and we classify these data into two categories according to their output probabilities (such as the data samples with high output probability and the data samples with low output probability), and the number of the two categories is the same (e.g., $\frac{n}{2}$). We extract the same number of data samples (e.g., η) from these two kinds of target data samples, and calculate the

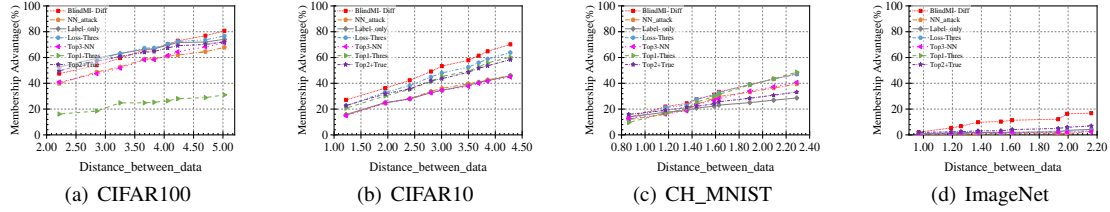


Figure 2. The effect of the distances between data samples of the target dataset on the Membership Advantage.

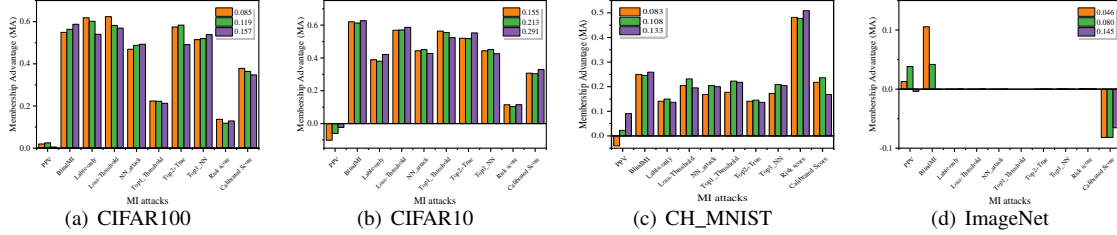


Figure 3. The effect of differential distance between two datasets on the Membership Advantage.

MMD [57] of these two categories target data samples (e.g., 2η). This calculation iterates until the MMDs are calculated for all samples in the target dataset, and we calculate a total of $\frac{n}{2\eta}$ groups of MMDs. According to the calculated $\frac{n}{2\eta}$ groups of MMDs of the target dataset, we rank these $\frac{n}{2\eta}$ groups MMDs and construct the distance distributions of data samples in the target dataset obey normal, uniform and bernoulli distributions, respectively. **Step 2: Calculate the distance between data samples of the target dataset (CV2) (Section 6.2).** For target datasets whose distance distribution of data samples obeying different distance distributions, we calculate the distance between data samples of the target dataset by the MMD method. **Step 3: Calculate the differential distance between two datasets (CV3) (Section 6.3).** Next, we generate a dataset with nonmembers via transforming existing samples into new samples or directly using the test data [14], and then we compute the differential distance between two datasets (i.e., the target dataset and a generated dataset with only nonmembers) before and after a data example (i.e., a data example with high output probability and a data example with low output probability) is moved from the target dataset to the nonmember dataset. **Step 4: Set the ratios of the samples that are made no inferences by an MI attack (CV4) (Section 6.4).** Finally, we set different ratios of the samples that are made no inferences by an MI attack for image datasets (i.e., 20%, 40%, 45% and 49%) and text datasets (i.e., 2%, 4%, 10% and 12%) as the prior Privacy Risk Scores-based [52] and the Shapley Values-based MI attacks [54].

After achieving these four steps, we use the four calculated CVs to build the evaluation scenarios (ESs), and each ES consists of four CVs, and we study a group level evaluation, where the concept of group is that a group consists of

multiple ESs, only one CV changes in a group and the other three CVs remain unchanged and the values of other three CVs must correspond to the same (see Section 6), and we make comprehensive evaluations of the existing MI attacks through the 10 typical evaluation metrics (Section 5.2.2). In this work, we have identified three principles for the proposed “comparing different MI attacks” methodology, and we have designed and implemented the MIBench benchmark with 84 ESs for each dataset. In total, we have used our benchmark to fairly and systematically compare 15 state-of-the-art MI attack algorithms (shown in Table 1) across 588 ESs, and these ESs cover 7 widely used datasets and 7 representative types of models.

4. Principles for better Explaining the attack Comparative Evaluation Results

4.1. Principle 1: The Two Primary Factors are Necessary but Insufficient

The two primary factors, i.e., the kind of data in the target dataset and the type of the target model, are necessary but insufficient to let a “comparing different MI attacks” methodology have desirable ability to explain the comparative evaluation results.

In order to incorporate these two factors in evaluating attack effectiveness, all the existing works use multiple target datasets and multiple types (e.g., MLP, ResNet, DenseNet) of target models. However, we find that even if the employed metrics are appropriate, the comparison results can still suffer from poor explanations. For example, researchers have already noticed the following: (a1) One MI attack algorithm could suffer from fairly different

TABLE 2. THE EVALUATION RESULTS OF THE TARGET DATASETS OBEYING DIFFERENT DISTANCE DISTRIBUTIONS OF DATA SAMPLES IN THE TARGET DATASET, ACCORDING TO TEN EVALUATION METRICS SUCH AS ACCURACY, PRECISION, RECALL, F1-SCORE, FNR, FPR, MA, AUC, TPR @ 0.01% FPR (T@0.01%F) AND THE THRESHOLD AT MAXIMUM MA (THRES@MAX MA).

Dataset	DisDistr.	DisBD.	DiffDis.	RatNoI.	Metric	Membership Inference Attack Algorithms														
						BlindMI -w	BlindMI -w/o	BlindMI -1CLASS	NN attack	Label -only	Loss -Thres	Top3-NN attack	Top1-Thres attack	Top2+True attack	Risk Scores attack	PPV attack	Calibrated Score	Shapley Values	Distillation -based Thre.	LIRA attack
CIFAR100	normal	2.893	0.085	20%	accuracy	73.23%	74.50%	68.88%	73.06%	81.13%	98.50%	75.94%	76.13%	96.38%	89.40%	51.56%	74.44%	52.75%	54.50%	53.54%
					precision	81.59%	82.82%	61.99%	65.57%	72.94%	97.95%	70.38%	89.49%	98.85%	83.43%	57.14%	67.16%	43.48%	54.20%	52.59%
					recall	73.00%	70.22%	93.46%	94.23%	97.44%	98.96%	91.59%	69.94%	94.02%	98.31%	12.50%	95.63%	56.82%	72.44%	64.86%
					f1-score	75.35%	76.00%	74.54%	77.33%	83.42%	98.45%	79.60%	78.51%	96.38%	90.26%	20.51%	78.91%	49.26%	62.00%	58.09%
					FNR	27.00%	29.78%	6.54%	5.77%	2.56%	1.04%	8.41%	30.06%	5.98%	1.69%	87.50%	4.38%	43.18%	27.56%	35.14%
					FPR	18.13%	19.71%	54.51%	47.07%	34.39%	1.93%	40.51%	13.62%	1.15%	19.52%	9.38%	46.75%	50.00%	64.36%	57.63%
					MA	54.88%	50.51%	38.95%	47.16%	63.05%	97.03%	51.07%	56.32%	92.87%	78.79%	3.13%	48.88%	6.82%	8.08%	7.24%
					AUC	0.790	0.747	0.695	0.846	0.810	0.025	0.840	0.492	0.960	0.225	0.012	0.152	0.100	0.538	0.456
					T@0.01%F	0.014%	0.013%	0.011%	0.26%	0.00%	0.00%	0.12%	0.00%	0.12%	0.00%	0.63%	0.00%	0.00%	0.00%	0.74%
					Thres@max MA	-	-	0.900	-	-	1.985	-	0.623	-	-2.98e ⁻³	0.640	1e ⁻⁶	-7.22e ⁻⁷	0.031	4.609
	uniform	2.893	0.085	20%	accuracy	71.19%	73.31%	69.56%	74.25%	79.88%	98.13%	76.56%	76.81%	97.25%	89.42%	53.38%	72.25%	51.91%	53.94%	45.56%
					precision	81.44%	79.49%	62.94%	67.03%	71.91%	97.47%	70.77%	83.42%	98.60%	84.05%	57.85%	65.61%	43.13%	53.38%	44.98%
					recall	68.88%	70.32%	93.29%	94.18%	97.22%	98.72%	91.48%	73.30%	95.93%	97.30%	24.88%	93.50%	66.35%	71.11%	57.29%
					f1-score	73.86%	74.63%	75.17%	78.32%	82.67%	98.09%	79.81%	78.03%	97.25%	90.20%	34.79%	77.11%	52.27%	60.98%	50.39%
					FNR	31.13%	29.68%	6.71%	5.82%	2.78%	1.28%	8.52%	26.70%	4.07%	2.70%	75.13%	6.50%	33.65%	28.89%	42.71%
					FPR	17.00%	22.91%	53.58%	45.19%	37.04%	2.44%	38.73%	18.69%	1.39%	18.47%	18.13%	49.00%	57.59%	63.67%	65.39%
					MA	51.88%	47.41%	39.71%	48.99%	60.18%	96.28%	52.75%	54.61%	94.53%	78.84%	6.75%	44.50%	8.75%	7.44%	-8.10%
					AUC	0.772	0.734	0.699	0.840	0.820	0.023	0.833	0.336	0.980	0.223	0.020	0.132	0.090	0.534	0.541
					T@0.01%F	0.014%	0.013%	0.010%	0.43%	0.00%	0.00%	0.13%	0.00%	0.10%	0.00%	0.88%	0.00%	0.00%	0.00%	1.53%
					Thres@max MA	-	-	0.900	0.220	-	1.984	-	0.717	-	-3.02e ⁻³	0.560	1e ⁻⁶	-5.49e ⁻⁶	0.014	4.538
	bernoulli	2.893	0.085	20%	accuracy	72.78%	75.50%	69.81%	74.56%	80.94%	80.38%	75.94%	75.19%	78.50%	89.68%	50.81%	71.69%	54.61%	51.00%	49.88%
					precision	81.29%	78.37%	63.54%	67.75%	73.37%	96.25%	69.74%	89.12%	93.96%	53.51%	64.87%	43.92%	50.75%	50.33%	
					recall	70.88%	74.11%	93.00%	93.75%	97.12%	73.06%	91.63%	69.70%	98.13%	98.11%	12.38%	94.63%	58.48%	67.37%	56.19%
					f1-score	74.90%	76.18%	75.49%	78.66%	83.59%	83.06%	79.20%	78.22%	92.03%	90.48%	20.10%	76.97%	50.17%	57.89%	53.10%
					FNR	29.13%	25.89%	7.00%	6.25%	2.88%	26.94%	8.37%	30.30%	1.88%	1.89%	87.63%	5.38%	41.52%	32.63%	43.81%
					FPR	17.13%	22.94%	53.37%	44.63%	35.25%	5.49%	39.75%	15.08%	41.13%	18.75%	10.75%	51.25%	47.88%	65.37%	56.57%
					MA	53.758%	51.17%	39.62%	49.12%	61.87%	67.56%	51.88%	54.62%	57.00%	79.36%	1.63%	43.38%	10.60%	2.00%	-0.38%
					AUC	0.782	0.755	0.698	0.850	0.810	0.032	0.840	0.106	0.880	0.234	0.012	0.132	0.107	0.505	0.514
					T@0.01%F	0.018%	0.015%	0.01%	0.28%	0.00%	0.00%	0.13%	0.00%	0.10%	0.00%	0.50%	0.00%	0.00%	0.00%	0.74%
					Thres@max MA	-	-	0.900	-	0.370	1.385	66.10%	0.550	-	-3.10e ⁻³	0.640	0.132	-8.23e ⁻¹¹	0.012	4.538

DisDistr.: the distance distribution of data samples in the target dataset; *DisBD.*: the distance between data samples of the target dataset;

DiffDis.: the differential distance between two datasets; *RatNoI.*: the ratio of the samples that are made no inferences by an MI attack.

evaluation results (i.e., metric measurements) against different target datasets: it is usually difficult to explain the lack of coherence cross datasets. In many cases, although the different target datasets have different data semantics (e.g., CIFAR100 holds 100 kind of data, while CH-MNIST holds 8 kind of data), strong correlation between the data semantics and the evaluation results is hard to identify. (a2) MI attack A is more effective than attack B against target dataset D1, but attack B is more effective than attack A against target dataset D2. In such situations, it is usually very difficult to draw general conclusions on when attack A would be more effective and when attack B would be more effective. For example, the Top2+True [14] attack (e.g., MA=43.71%) is more effective than the NN_attack [8] (e.g., MA=34.51%) against CIFAR10, whereas the NN_attack [8] (e.g., MA=0.008%) is more effective than Top2+True [14] attack (e.g., MA=0.003%) against ImageNet. (a3) Many MI attacks suffer from high FPR (see Figure 8) and low precision (see Figure 9) against widely-used test datasets (e.g., NN_attack [8] (51.7%), Label-only [13] (50.5%) and BlindMI-Diff [14] (50.01%)). However, it is usually difficult to explain why higher precision is not achieved.

4.2. Principle 2: Distance Distribution of Data Samples in the Target Dataset Matters

Incorporating the following factor could substantially enhance the ability of a “comparing different MI attacks” methodology to explain the comparative evaluation results: (factor 1) the effectiveness of an MI attack could be highly

sensitive to the distance distribution of data samples in the target dataset.

From Table 2, we discover that the evaluation results of an MI attack are different when distance distributions of data samples in the target dataset obey different distance distributions (e.g., the MAs and the TPR @ 0.01% FPR of the Positive Predictive Value (PPV) attack [50] are 3.13%, 6.75%, 1.63% and 0.63%, 0.88%, 0.50% when the distance distribution of data samples in the target dataset obeys normal, uniform, and bernoulli distributions, respectively.)

4.3. Principle 3: Distance between Data Samples of the Target Dataset Matters

Incorporating the following factor could substantially enhance the ability of a “comparing different MI attacks” methodology to explain the comparative evaluation results: (factor 2) the effectiveness of an MI attack could be highly sensitive to the distances between data samples of the target dataset.

From Figure 2, we discover that the evaluation results of an MI attack are different when target datasets have different distances between data samples (e.g., the MAs of the NN attack [8] are 28.89%, 32.98% and 39.39% when the distance between data samples of the target dataset are 2.510, 3.813, 4.025, respectively).

4.4. Principle 4: Differential Distance between Two Datasets Matters

Incorporating the following factor could substantially enhance the ability of a “comparing different MI attacks”

TABLE 3. THE DESCRIPTION OF DIFFERENT DATASETS USED IN OUR EVALUATION.

Dataset	Description	# of class	Resolution	# Epochs(target model)	$\mathcal{T}\mathcal{S}_t$	$\mathcal{T}\mathcal{S}_s$	\mathcal{D}_{t1}	\mathcal{D}_{t2}	\mathcal{D}_{t3}	\mathcal{D}_{t4}
CH_MNIST	histological images	8	64×64	(pre-trained + 15) or 150	2,500	2,500	5,000	800	800	800
CIFAR10	image classification	10	32×32	(pre-trained + 30) or 150	10,000	10,000	20,000	2,000	2,000	2,000
CIFAR100	image classification	100	32×32	(pre-trained + 30) or 150	10,000	10,000	20,000	2,000	2,000	2,000
ImageNet	image classification	200	64×64	(pre-trained + 30) or 150	10,000	10,000	20,000	2,000	2,000	2,000
Location30	text classification	30	64×64	(pre-trained + 30) or 150	1,000	1,000	2,000	500	500	500
Purchase100	text classification	100	64×64	(pre-trained + 30) or 150	19,732	19,732	39,464	2,000	2,000	2,000
Texas100	text classification	100	64×64	(pre-trained + 30) or 150	10,000	10,000	20,000	1,560	1,560	1,560

$\mathcal{T}\mathcal{S}_t$ and $\mathcal{T}\mathcal{S}_s$ are the training datasets of the target and shadow models, respectively. \mathcal{D}_{t1} is the target dataset that doesn't obey any distribution, \mathcal{D}_{t2} - \mathcal{D}_{t4} are the target datasets obeying normal, uniform and bernoulli distributions, respectively.

methodology to explain the comparative evaluation results: (factor 3) the effectiveness of an MI attack could be highly sensitive to the differential distance (i.e., MMD [57]) before and after a data example is moved from the target dataset to a generated dataset with only nonmembers.

From Figure 3, we find that the evaluation results of an MI attack are different when target datasets have different differential distances between two datasets (e.g., the MAs of the Calibrated Score attack [56] are 46.73%, 39.82% and 43.45% when the differential distances between two datasets are 0.085, 0.119, 0.157, respectively).

5. Evaluation Framework

In this section, we first introduce the experimental setup of our benchmark. Then, we propose the composition of the evaluation framework.

5.1. Experimental Setup

Implementation. In this paper, we utilize the Python 3.7 to achieve our evaluations. And nonmembers utilized in our experiments is the same as [14].

Models. We adopt the same model architectures and hyperparameters as prior BlindMI-Diff attack [14], which are defined in table 4. We also adopt a multilayer perceptron (MLP) model that has at most seven dense layers (e.g., 8192, 4096, 2048, 1024, 512, 256 and 128), and an additional Softmax layer. The standard CNN architectures and hyperparameters are the same as the prior black MI attack [8]. We also utilize the three kinds of popular DNNs (e.g., VGG, ResNet and DenseNet), which are standard architectures with pre-trained parameters from ImageNet.

Target Model. Given a dataset, we randomly select a target model from the target model column of Table 4, and train the target model with the specified hyperparameters.

Shadow Model. For black-box attacks, we randomly select a shadow model architecture from the shadow model column of Table 4. For the gray/white-box settings, we select the same architectures as the given target model as our shadow models' architectures.

Datasets. We utilize seven datasets (as shown in Table 3) to perform the comprehensive evaluations of the existing MI attacks. We select half members and half nonmembers in each target dataset, and the details are shown in the Appendix A.

TABLE 4. THE DESCRIPTION OF SETTINGS ON TARGET AND SHADOW MODELS' ARCHITECTURES AND HYPERPARAMETERS.

ModArch.	# of layers	target model		shadow model	
		MaxEpoch.	LNRate.	MaxEpoch.	LNRate.
MLP	[3-7] dense	e_m	$5e-5$	$[0.3-2]e_m$	$1e-4/1e-5$
StandDNN	2	e_m	$5e-5$	$0.5e_m$	$1e-4$
VGG16	16	$e_p^* + e_m^{**}$	$5e-5$	$e_p + 0.6e_m$	$5e-5$
VGG19	19	$e_p + e_m$	$5e-5$	$e_p + 1.5e_m$	$5e-5$
ResNet50	50	$e_p + e_m$	$5e-5$	$e_p + 0.2e_m$	$5e-5$
ResNet101	101	$e_p + e_m$	$5e-5$	$e_p + 0.3e_m$	$1e-4$
DenseNet121	121	$e_p + e_m$	$5e-5$	$e_p + e_m$	$1e-4$

e_m is the maximum epochs of target model for each dataset in table 3; e_p is the epoch of a pre-trained weight on the ImageNet dataset.

5.2. The Composition of the Evaluation Framework

The primary design goal of our benchmark, called **MIBench**, is to meet *all* of above-mentioned 4 requirements (see Section 1). Our benchmark consists not only the evaluation metrics (Section 5.2.2), but also the evaluation scenarios (Section 5.2.1). We design the evaluation scenarios from the **four perspectives** mentioned in Section 1, and the ratio of the samples that are made no inferences by an MI attack. Moreover, each perspective corresponds to a control variable and so there are in total four **control variables** in our evaluation scenarios. The evaluation metric module consists of ten typical evaluation metrics.

5.2.1. Part I: Evaluation Scenarios. Since fine-grained attacks make no inferences on certain data examples, it seems unfair to use the same number of data examples when comparing indiscriminate attack algorithms and fine-grained attack algorithms (shown in Figure 5).

The inaccurate and unfair evaluation results shown in Figure 5, Principle 2 (Section 4.2), Principle 3 (Section 4.3) and Principle 4 (Section 4.4) indicate that a good evaluation framework should have at least 4 control variables, consisting of the distance distribution of data samples in the target dataset (CV1), the distance between data samples of the target dataset (CV2), the differential distance between two datasets (CV3), and the ratio of the samples that are made no inferences by an MI attack (CV4).

The four control variables adopted in our evaluation scenarios (as shown in Figure 4) are as follows: **Control Variable 1:** {C100_N, C100_U, C100_B; C10_N, C10_U, C10_B; CH_N, CH_U, CH_B; I_N, I_U, I_B, L30_N, L30_U, L30_B; P100_N, P100_U, P100_B; T100_N,

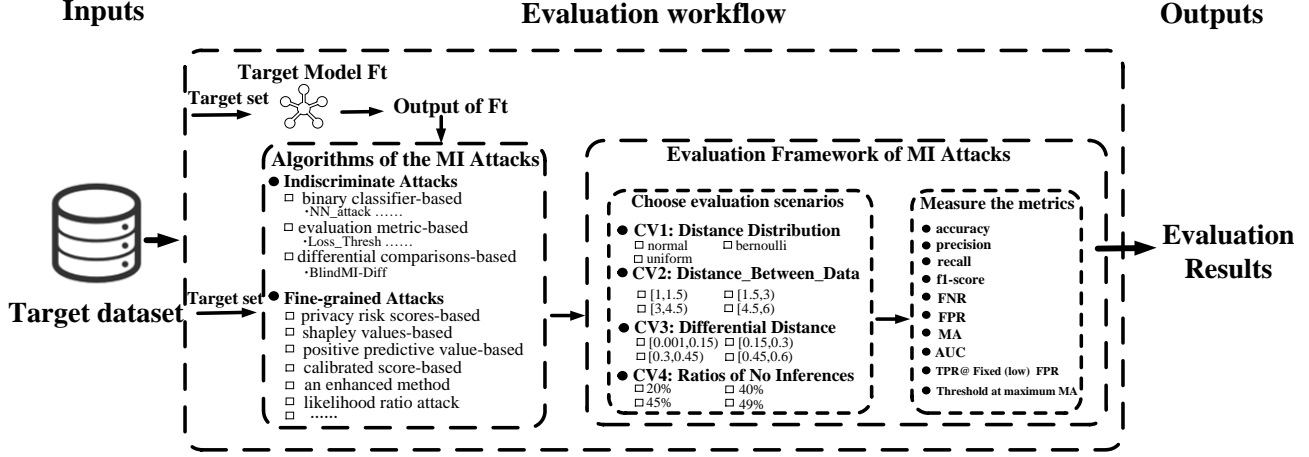


Figure 4. The Evaluation Workflow of the Membership Inference Attacks.

T100_U, T100_B}; **Control Variable 2:** {1.225, 1.24, ..., 6.250}; **Control Variable 3:** {0.001, 0.002, ..., 0.500}; **Control Variable 4:** {2%, 4%, 10%, 12%, 20%, 40%, 45%, 49%}. Based on the four control variables, we build 84 evaluation scenarios for each dataset, and the 84 evaluation scenarios of the CIFAR100 are shown in Table 5.

5.2.2. Part II: Evaluation Metrics. We mainly use attacker-side accuracy, precision, recall, f1-score, false positive rate (FPR), false negative rate (FNR), membership advantage (MA), the Area Under the Curve (AUC) of attack Receiver Operating Characteristic (ROC) curve [55], TPR @ fixed (low) FPR [55], threshold at maximum MA, as our evaluation metrics (as shown in Figure 4). Specifically, *accuracy* is the percentage of data samples with correct membership predictions by MI attacks; *precision* represents the ratio of real-true members predicted among all the positive membership predictions made by an adversary; *recall* demonstrates the ratio of true members predicted by an adversary among all the real-true members; *f1-score* is the harmonic mean of precision and recall; *FPR* is the ratio of nonmembers are erroneously predicted as members; *FNR* is the difference of the 1 and recall (e.g., $FNR = 1 - \text{recall}$); *MA* is the difference between the true positive rate and the false positive rate (e.g., $MA = \text{TPR} - \text{FPR}$ [13]); *AUC* is computed as the Area Under the Curve of attack ROC in logarithmic scale; *TPR @ fixed (low) FPR* is an attack’s true-positive rate at (fixed) low false-positive rates in logarithmic scale; and the *threshold at maximum MA* is a threshold to achieve maximum MA.

6. Using MIBench to Compare Different MI Attacks

The high-level idea for using the proposed benchmark is the controlled variable approach, where only one control variable (CV) is allowed to change at a time and the other

three CVs are left unchanged, and then the evaluation results of the different MI attacks in this case are tested. Our evaluation aims to answer the following Research Questions (RQs). **RQ1:** Whether target datasets obeying different distance distributions of data samples have notable effects on the (effectiveness) ranking of state-of-the-art MI attacks when other three CVs keep the same values? **RQ2:** Whether target datasets that have different distances between data samples have notable effects on the (effectiveness) ranking? **RQ3:** Whether target datasets that have different differential distances between two datasets have notable effects on the (effectiveness) ranking? **RQ4:** Whether target datasets that have different ratios of the samples that are made no inferences by an MI attack have notable effects on the (effectiveness) ranking?

In our experiments, the target dataset sizes are shown in Table 3. We first divide the target dataset into small batches of 20 data samples as the prior BlindMI-Diff attack [14], then we calculate the MMD of the output probabilities through target models by Equation 1. Next, we construct and calculate 4 CVs as described in Section 5.2.1. Finally, we use our benchmark to fairly and systematically compare 15 state-of-the-art MI attack algorithms (see Table 1) across 588 evaluation scenarios (84 evaluation scenarios for each dataset (see Table 5)), and study how every CV affects the evaluation results. Each attack is performed ten times with a new target and shadow model with different training datasets, model architectures and hyperparameters each time, and we obtain the average values of 10 evaluation metrics together with the standard error of the mean among the thirteen attacks. We perform experiments on CIFAR100, CIFAR10, CH_MNIST and ImageNet with seven model architectures described in Section 5.1, and for Location30, Purchase100 and Texas100, we use fully connected neural networks with 4 hidden layers, and the numbers of neurons for hidden layers are 1024, 512, 256, and 128, respectively. We use Tanh as the activation function on Purchase100 and

TABLE 5. EVALUATION SCENARIOS OF CIFAR100.

ESN.	DisDistr.	DisBD.	DiffDis.	RatNoI.	ESN.	DisDistr.	DisBD.	DiffDis.	RatNoI.	ESN.	DisDistr.	DisBD.	DiffDis.	RatNoI.	ESN.	DisDistr.	DisBD.	DiffDis.	RatNoI.
ES01	Normal	2.893	0.085	20%	ES22	Normal	4.325	0.085	40%	ES43	Uniform	3.813	0.119	45%	ES64	Bernoulli	2.893	0.157	49%
ES02	Normal	2.893	0.085	40%	ES23	Normal	4.325	0.085	45%	ES44	Uniform	3.813	0.119	49%	ES65	Bernoulli	3.813	0.085	20%
ES03	Normal	2.893	0.085	45%	ES24	Normal	4.325	0.119	40%	ES45	Uniform	3.813	0.157	20%	ES66	Bernoulli	3.813	0.085	40%
ES04	Normal	2.893	0.119	40%	ES25	Normal	4.325	0.119	45%	ES46	Uniform	3.813	0.157	40%	ES67	Bernoulli	3.813	0.085	45%
ES05	Normal	2.893	0.119	45%	ES26	Normal	4.325	0.119	49%	ES47	Uniform	3.813	0.157	45%	ES68	Bernoulli	3.813	0.085	49%
ES06	Normal	2.893	0.119	49%	ES27	Normal	4.325	0.157	45%	ES48	Uniform	3.813	0.157	49%	ES69	Bernoulli	3.813	0.119	20%
ES07	Normal	2.893	0.157	45%	ES28	Normal	4.325	0.157	49%	ES49	Uniform	4.325	0.085	20%	ES70	Bernoulli	3.813	0.119	40%
ES08	Normal	2.893	0.157	49%	ES29	Uniform	2.893	0.085	20%	ES50	Uniform	4.325	0.085	40%	ES71	Bernoulli	3.813	0.119	45%
ES09	Normal	3.813	0.085	20%	ES30	Uniform	2.893	0.085	40%	ES51	Uniform	4.325	0.085	45%	ES72	Bernoulli	3.813	0.119	49%
ES10	Normal	3.813	0.085	40%	ES31	Uniform	2.893	0.085	45%	ES52	Uniform	4.325	0.119	40%	ES73	Bernoulli	3.813	0.157	20%
ES11	Normal	3.813	0.085	45%	ES32	Uniform	2.893	0.119	40%	ES53	Uniform	4.325	0.119	45%	ES74	Bernoulli	3.813	0.157	40%
ES12	Normal	3.813	0.085	49%	ES33	Uniform	2.893	0.119	45%	ES54	Uniform	4.325	0.119	49%	ES75	Bernoulli	3.813	0.157	45%
ES13	Normal	3.813	0.119	20%	ES34	Uniform	2.893	0.119	49%	ES55	Uniform	4.325	0.157	45%	ES76	Bernoulli	3.813	0.157	49%
ES14	Normal	3.813	0.119	40%	ES35	Uniform	2.893	0.157	45%	ES56	Uniform	4.325	0.157	49%	ES77	Bernoulli	4.325	0.085	20%
ES15	Normal	3.813	0.119	45%	ES36	Uniform	2.893	0.157	49%	ES57	Bernoulli	2.893	0.085	20%	ES78	Bernoulli	4.325	0.085	40%
ES16	Normal	3.813	0.119	49%	ES37	Uniform	3.813	0.085	20%	ES58	Bernoulli	2.893	0.085	40%	ES79	Bernoulli	4.325	0.085	45%
ES17	Normal	3.813	0.157	20%	ES38	Uniform	3.813	0.085	40%	ES59	Bernoulli	2.893	0.085	45%	ES80	Bernoulli	4.325	0.119	40%
ES18	Normal	3.813	0.157	40%	ES39	Uniform	3.813	0.085	45%	ES60	Bernoulli	2.893	0.119	40%	ES81	Bernoulli	4.325	0.119	45%
ES19	Normal	3.813	0.157	45%	ES40	Uniform	3.813	0.085	49%	ES61	Bernoulli	2.893	0.119	45%	ES82	Bernoulli	4.325	0.119	49%
ES20	Normal	3.813	0.157	49%	ES41	Uniform	3.813	0.119	20%	ES62	Bernoulli	2.893	0.119	49%	ES83	Bernoulli	4.325	0.157	45%
ES21	Normal	4.325	0.085	20%	ES42	Uniform	3.813	0.119	40%	ES63	Bernoulli	2.893	0.157	45%	ES84	Bernoulli	4.325	0.157	49%

ESN.: the number of the Evaluation Scenarios; *DisDistr.*: the distance distribution of data samples in the target dataset; *DisBD.*: the distance between data samples of the target dataset; *DiffDis.*: the differential distance between two datasets; *RatNoI.*: the ratio of the samples that are made no inferences by an MI attack.

Texas100 datasets, and ReLU on the Location30. For all MI attacks, we evaluate them with metrics in Section 5.2.2, and for the fine-grained MI attacks based on thresholds (e.g., Shapley Values [54] and Risk Scores [52]), we report different thresholds for different classes at maximum MA (e.g., 100 thresholds on different classes on CIFAR100) and other MI attacks that use a single threshold for all classes (e.g., Loss-Threshold [13], Top1-Threshold [9], PPV [50], Calibrated Score [56], Distillation-based Thre. [53] and LiRA [55]), we report the thresholds at maximum MA. All evaluation results of MIBench are shown in the <https://github.com/MIBench/MIBench.github.io/blob/main/README.md>.

Because of the (simplified) 84 evaluation scenarios, for each dataset, we select three distances among all distances between data samples under different distance distributions and three distances among all differential distance between two datasets, respectively. And the distances are the mean distance of the distance between data samples (or the differential distance between two datasets) and the two distances equally divided on the the left and right sides, respectively. For example, the three distances between data samples (differential distances between two datasets) selected on the CIFAR100 are 2.893, 3.813, 4.325 (0.085, 0.119, 0.157), respectively. (see Table 9 in the Appendix C).

6.1. RQ1: Effect of the Distance Distribution of Data Samples in the Target Dataset

Methodology. For a target dataset, we first input all data samples (e.g., n) in the target dataset to the target model and get the corresponding output probabilities, and we classify these data into two categories according to their output probabilities (such as the data samples with high output probability and the data samples with low output probability), and the number of the two categories is the same (e.g., $\frac{n}{2}$). We extract the same number of data samples (e.g., η) from these two kinds of target data samples, and utilize Equation 1 to calculate the MMD [57] of these two categories target data samples' output probabilities through target models (e.g., 2η).

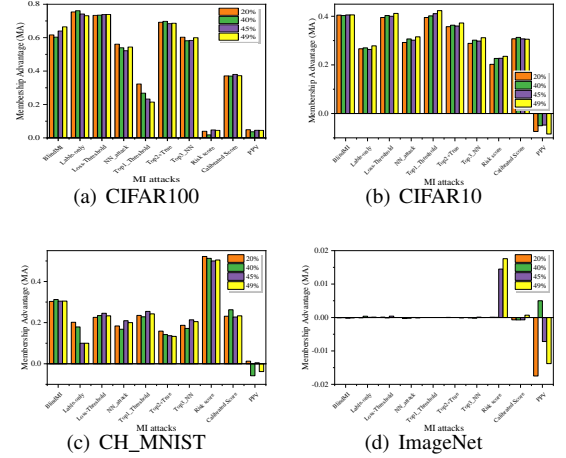


Figure 5. The effect of the ratio of the samples that are made no inferences by an MI attack.

$$\text{MMD}[\mathcal{P}_p, \mathcal{P}_q] = \left\| \frac{1}{n_p} \sum_{i=1}^{n_p} \phi(\mathcal{P}_i) - \frac{1}{n_q} \sum_{j=1}^{n_q} \phi(\mathcal{P}_j) \right\|_v \quad (1)$$

where $\mathcal{P}_i \in \mathcal{P}_p$ and $\mathcal{P}_j \in \mathcal{P}_q$, p and q are data samples with high output probability and data samples with low output probability of the target dataset, respectively. And n_p and n_q are the size of \mathcal{P}_p and \mathcal{P}_q , respectively. $\phi(\cdot)$ is a feature space map from the probability of the target model to the Reproducing Kernel Hilbert Space (RKHS) [58], namely $k \mapsto \nu$. And most commonly used is a Gaussian kernel function, namely $k(\mathcal{P}_p, \mathcal{P}_q) = \langle \phi(\mathcal{P}_p), \phi(\mathcal{P}_q) \rangle = \exp(-\|\mathcal{P}_p - \mathcal{P}_q\| / (2\sigma^2))$.

This calculation of MMD is performed until the MMDs are calculated for all samples in the target dataset, and we calculate a total of $\frac{n}{2\eta}$ groups of MMDs. Next, according to the calculated $\frac{n}{2\eta}$ groups of MMDs of the target dataset, we first sort these $\frac{n}{2\eta}$ groups MMDs in ascending order,

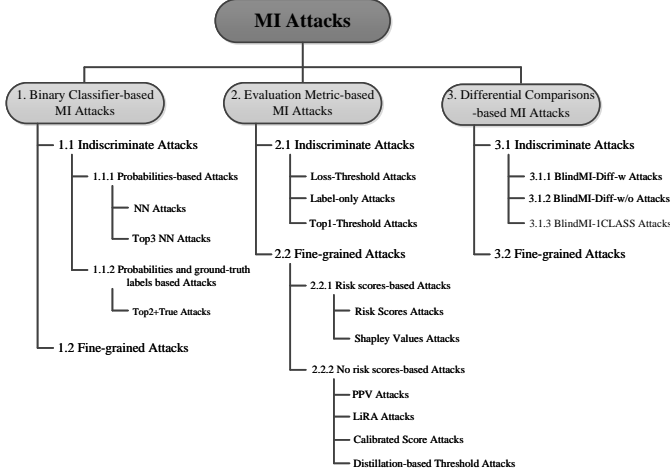


Figure 6. The Classification of the Membership Inference Attacks.

namely $MMD = \{MMD_1, \dots, MMD_{n/2\eta}\}$. Then, we construct the distance distributions of data samples in the target dataset as normal, uniform and bernoulli distributions, respectively. (a) **Normal Distribution.** We select some MMDs from the calculated $\frac{n}{2\eta}$ groups of MMDs of the target dataset to construct a set of MMDs, $\{MMD_1, \dots, MMD_h\}$ ($1 \leq h \leq n/2\eta$), which obeys a normal distribution, that is, $\{MMD_1, \dots, MMD_h\} \sim N(\mu, \sigma^2)$, where μ and σ are the mean and variance of the normal distribution, respectively. (b) **Uniform Distribution.** We assume two parameters a and b , and the $MMD_1 \leq a \leq b \leq MMD_{n/2\eta}$. We select MMD_i from the calculated $\frac{n}{2\eta}$ groups of MMDs of the target dataset, and $a \leq MMD_i \leq b$ and divide the selected MMDs, $\{MMD_1, \dots, MMD_s\}$ ($1 \leq s \leq n/2\eta$), in the distance intervals $[a, b]$ equally into several parts (e.g., γ) and the number of MMD distance groups in each MMD distance part is equal (e.g., s/γ). Therefore, the selected MMDs obeys a uniform distribution of parameters s/γ on $[a, b]$. (c) **Bernoulli Distribution.** We select a distance threshold (e.g., ϵ) in the calculated $\frac{n}{2\eta}$ groups of MMDs of the target dataset as the split point of the Bernoulli distribution, and if the selected MMD_i is smaller than the selected distance threshold ϵ , we regard the incident as a success, otherwise a failure. Specially, we select some MMDs, $\{MMD_1, \dots, MMD_r\}$ ($1 \leq r \leq n/2\eta$) from the calculated $\frac{n}{2\eta}$ groups of MMDs of the target dataset, and construct these selected MMDs (e.g., $\{MMD_1, \dots, MMD_r\}$) obey Bernoulli distribution with a parameter p , where the ratio of MMDs greater than the distance threshold ϵ is p and the ratio of MMDs less than ϵ is $(1-p)$.

In our experiments, for a target dataset on each dataset (see \mathcal{D}_{t1} in Table 3), we first input all data samples (e.g., 20,000 on CIFAR100) in the target dataset to the target model and get the corresponding output probabilities, and we classify these data into two categories according to their output probabilities (such as the data samples with high output probability and the data samples with low output

probability), and the number of the two categories is the same (e.g., 10,000). We extract the same number of data samples (e.g., 10), as the prior BlindMI-Diff attack [14], from these two kinds of target data samples, and combine them into small batches of 20 data samples and utilize Equation 1 to calculate the MMD [57] of them. And we in total get 1000 MMDs, and original distance distribution of the 1000 MMDs on CIFAR100 is shown as Figure 13(a), and from the Figure 13(a) we find that the original distance distribution of the 1000 MMDs on CIFAR100 is approximately normal distribution. When the original distance is within a certain range, the original distance distribution of the MMDs on CIFAR100 dataset is approximately uniform distribution (see Figure 14(h)). We select different distance thresholds of the 1000 MMDs on target CIFAR100 dataset, and find that the distance of the 1000 MMDs on CIFAR100 dataset is Bernoulli distribution shown in Table 10. We find the similar phenomenon in other six target datasets, and the results are shown in the Appendix B.

Because of the fair evaluation of the attack results under these three distributions, we chose an equal number of samples to calculate the MMDs (see $\mathcal{D}_{t2}-\mathcal{D}_{t4}$ in Table 3), and we select equal number of MMDs (e.g., 100 MMDs on CIFAR100) to construct the distance distribution of data samples in target datasets as normal, uniform and bernoulli distributions, respectively (see Figure 14 in Appendix B).

Results. We verify the evaluation results of 15 state-of-the-art MI attacks when only the distance distribution of data samples in the target dataset (CV1) is allowed to change and other three CVs (see Section 5.2.1) are left unchanged. From Table 2 and Figure 15, we discover that the evaluation results of an MI attack are different when target datasets obey different distance distributions. We observe that the ranking results of a particular MI attack (i.e. Loss-Threshold [13] (Class 2.1 see Figure 6)) remain **unchanged** across almost all the ESs in a particular group (i.e., when only the CV1 changed and other three CVs remained the same, the Loss threshold based attack [13] is 85.17% of the top three most effective attacks). This indicates that the corresponding tuning variable probably does not affect the MI attack. To confirm this conclusion, we look into the algorithm of the MI attack and find the following: the Loss threshold-based attack [13] required a shadow model and computed the average cross-entropy loss of all training samples in the shadow model to distinguish members. Therefore, when only the CV1 changes and other three CVs remain the same, it does not affect the average cross-entropy loss of the Loss threshold based attack [13], and thus has little effect on evaluation results.

We find that the Top1-Threshold based attack [9] (Class 2.1 see Figure 6)) is most affected when only the CV1 changes, other three CVs remain the same, for example, for one particular ES01 on Purchase100 could result in the following ranking: Class 2.1 (except for the Label-only, Loss Threshold attacks) > Class 3.1.2 > Class 2.2.1 (except for the Shapley values attack) > Class 1.1.2 > Class 1.1.1 (except for the Top3_NN attack) > Class 2.2.2 (except for the Calibrated Score, LiRA and PPV attacks) > Class

3.1.1 > Class 3.1.3, and for another particular ES29 on Purchase100 could result in the following ranking: Class 3.1.2 > Class 1.1.2 > Class 2.2.1 (except for the Shapley values attack) > Class 1.1.1 (except for the Top3_NN attack) > Class 2.1 (except for the Loss Threshold attack) > Class 2.2.2 (except for the LiRA and PPV attacks) > Class 3.1.1 > Class 3.1.3. The reason is that the Top1-Threshold based attack [9] needs some extra nonmembers to get the nonmember threshold to infer members, and the evaluation results of Top1_Threshold attacks depends on the choice of the nonmembers, and when only CV1 changes and the nonmembers remain unchanged, may cause the selected nonmembers to be unable to effectively distinguish between members and nonmembers of different distance distributions of data samples in the target dataset.

We also observe that the ranking order between two particular MI attacks (i.e. Top3-NN attack [9] and NN_attack [8] (Class 1.1.1)) remain **unchanged** across almost all the ESs in a particular group. This indicates that the ranking order is independent of the control variable. In addition, this indicates that the ranking order is to certain extent determined by the three non-tuning factors. We look into the values of the three non-tuning factors, and we find that the ranking order between Top3-NN attacks and NN_attacks is Top3_NN > NN_attack when only the CV1 changes and other three CVs remain the same, while the ranking order of them is NN_attack > Top3_NN when only the CV2 changes and the other three variables remain the same. The reason is that Top3-NN attacks and NN_attacks are mainly based on the output probability of the target model, so it hardly affects the ranking order of them when only the CV1 changes, which does not effect the output probability of the target model; and changing only the CV2 will change the distance between the data samples with high output probability and data samples with low output probability of the target dataset to some extent, this will affect the attack decision, and finally make the ranking order of the two attacks change. Meanwhile, from Figure 10, We find that the FNR is almost the same when the target datasets obeying different distance distributions of data samples in the target dataset.

[Observation] *The distance distributions of data samples in the target dataset have little effect on the FNR.*

6.2. RQ2: Effect of Distance between Data Samples of the Target Dataset

Methodology. For target datasets obeying different distance distributions, we first use the Equation 1 to calculate the distance between data samples (e.g., data samples with high output probability and data samples with low output probability classified in Section 6.1) of the target dataset. Then, we verify the evaluation results of 15 state-of-the-art MI attacks when only the distance between data samples (e.g., data samples with high output probability and data samples with low output probability) (CV2) of the target dataset is allowed to change and other three CVs (see Section 5.2.1) are left unchanged.

Results. From Figure 2, we discover that the MA of the MI attacks increases with the increase of the distance between data samples of the target dataset. Meanwhile, Table 7 also shows the similar results that the distance between data samples on ImageNet, CH_MNIST, CIFAR10 and CIFAR100 increases in turn, and the MA increases gradually. We observe that the ranking results of a particular MI attack (i.e. Top2+True attack [14] (Class 1.1.2 see Figure 6)) remain **unchanged** across almost all the ESs in a particular group (i.e., when only the CV2 changed and other three CVs remained the same, the Top2+True attack [14] is 70.83% of the top three to top five most effective attacks). This indicates that the corresponding tuning variable probably does not affect the MI attack. To confirm this conclusion, we look into the algorithm of the MI attack and find the following: Top2+True attacks [14] mainly combined the top two output probabilities of the target model and the ground-truth labels. Therefore, when only the CV2 changes and other three CVs remain the same, it does not affect the ground-truth labels of the target dataset, and thus has little effect on evaluation results of the Top2+True attacks [14].

We find that the Top3_NN attack [9] (Class 1.1.1 see Figure 6) is most affected when only CV2 changes, other three CVs remain the same, for example, for one particular evaluation scenario ES14 on CH_MNIST could result in the following ranking: Class 2.1 (except for the Label-only and Loss-Threshold attacks) > Class 2.2.1 (except for the Shapley values attack) > Class 1.1.1 (except for the NN attack) > Class 3.1.1 > Class 3.1.2 > Class 2.2.2 (except for the Distillation-based, PPV, LiRA attacks) > Class 1.1.2 > Class 3.1.3, and for another particular evaluation scenario ES24 on CH_MNIST could result in the following ranking: Class 2.1 (except for the Label-only and Loss-Threshold attacks) > Class 2.2.1 (except for the Shapley values) > Class 3.1.1 > Class 3.1.2 > Class 2.2.2 (except for the Distillation-based, PPV, LiRA attacks) > Class 1.1.1 (except for the NN attack) > Class 1.1.2 > Class 3.1.3. The reason is that the Top3_NN attack [9] mainly is based on the Top three output probability of the target model, and when only the CV2 changes, the difference between members and nonmembers could not be captured effectively by the Top3_NN attack, which will affect evaluation results.

We also observe that the ranking order between two particular MI attacks (i.e. LiRA attack [55] and PPV attack [50] (Class 2.2.2 see Figure 6)) remain **unchanged** across almost all the ESs in a particular group. This indicates that the ranking order is independent of the control variable. In addition, this indicates that the ranking order is to certain extent determined by the three non-tuning factors. We look into the values of the three non-tuning factors, and we find that the ranking order between LiRA attacks and PPV attacks is PPV > LiRA when only the CV2 changes and other three CVs remain the same, while the ranking order of them is LiRA > PPV when only CV4 changes and other three variables remain the same. The reason is that PPV attacks mainly considered the prior distribution of the data, and they classified a target data example as a member when its per-instance loss was larger than a decision threshold, and the

TABLE 6. THE MI ATTACKS THAT RANK OPPOSITE.

ARN.	Attack A	Attack B	EL.	RAR.	OAR.	dataset	RES.	MR.SMR.	ARN.	Attack A	Attack B	EL.	RAR.	OAR.	dataset	RES.	MR.SMR.
AR01	Risk score	Loss-Threshold	1+2	A > B	A < B	2+3+6	ES03:C100_N+2.893+0.085+45% ES01:C100_N+2.893+0.085+20% ES01:C100_N+2.893+0.085+20% ES21:C100_N+4.325+0.085+20%	CV4 40%	AR43	BlindMI-ICLASS	Top3_NN	3	A > B	A < B	1+4+6	ES63:C10_B+1.908+0.291+45% ES59:C10_B+1.908+0.155+45% ES68:C10_B+2.501+0.155+49% ES65:C10_B+2.501+0.155+20%	CV3 40%
AR02	Loss-Threshold	Label-Only	3	A > B	A < B	2	ES09:CH_M_N+1.355+0.083+20% ES12:CH_M_N+1.355+0.083+49%	CV4 40%	AR44	Risk score	PPV	5	A > B	A < B	1	ES13:C10_N+2.501+0.213+20% ES16:C10_N+2.501+0.213+49%	CV4 40%
AR03	Top2+True	Risk score	-	A > B	A < B	2+3+6	ES07:CH_M_N+0.954+0.133+45% ES27:CH_M_N+1.720+0.133+45%	CV2 40%	AR45	LiRA	Risk score	1	A > B	A < B	1	ES02:T100_N+0.530+0.038+4% ES04:T100_N+0.530+0.073+4%	CV3 40%
AR04	Label-Only	Top2+True	3	A > B	A < B	2+3	ES52:C10_U+3.472+0.213+40% ES32:C10_U+1.908+0.213+40%	CV2 40%	AR46	Calibrated Score	BlindMI-w	-	A > B	A < B	3+4+5+6+7	ES45:CH_M_U+1.355+0.133+20% ES48:CH_M_U+1.355+0.133+49%	CV4 40%
AR05	Top1_Threshold	Top2+True	3	A > B	A < B	1+2+3+6+7	ES46:C10_U+2.501+0.291+40% ES38:C10_U+2.501+0.155+40%	CV4 40%	AR47	Calibrated Score	Shapley values	-	A > B	A < B	3	ES83:CH_M_B+1.720+0.133+45% ES63:CH_M_B+0.954+0.133+45%	CV2 40%
AR06	BlindMI-w	Top2+True	3	A > B	A < B	1+2+3+4	ES56:CH_M_U+1.720+0.133+49% ES36:CH_M_U+0.954+0.133+49%	CV2 40%	AR48	Calibrated Score	Distillation-based	1	A > B	A < B	3	ES75:ImaN_B+1.130+0.145+45% ES67:ImaN_B+1.130+0.046+45%	CV3 40%
AR07	Top3_NN	Top2+True	3	A > B	A < B	1+2+3+5	ES07:C100_N+2.893+0.157+45% ES03:C100_N+2.893+0.085+45%	CV3 40%	AR49	BlindMI-w	Distillation-based	-	A > B	A < B	3+4	ES49:CH_M_U+1.720+0.083+20% ES29:CH_M_U+0.954+0.083+20%	CV2 40%
AR08	BlindMI-without	Top2+True	3	A > B	A < B	1+2+3	ES26:CH_M_N+1.720+0.108+49% ES06:CH_M_N+0.954+0.108+49%	CV2 40%	AR50	Top3_NN	Shapley values	-	A > B	A < B	3+4+5+7	ES49:L30_U+0.801+0.041+4% ES29:L30_U+0.570+0.041+4%	CV2 40%
AR09	NN_attack	Top2+True	3	A > B	A < B	1+2+3+4	ES02:P100_N+0.550+0.087+4% ES10:P100_N+0.625+0.087+4%	CV2 40%	AR51	Top3_NN	Distillation-based	-	A > B	A < B	3+4+5+7	ES07:T100_N+0.530+0.107+10% ES03:T100_N+0.530+0.038+10%	CV3 40%
AR10	Top1_Threshold	Label-only	3	A > B	A < B	2+6	ES07:C100_N+2.893+0.157+45% ES03:C100_N+2.893+0.085+45%	CV3 40%	AR52	BlindMI-without	Risk score	-	A > B	A < B	6+7	ES08:P100_N+0.550+0.156+12% ES06:P100_N+0.550+0.110+12%	CV3 40%
AR11	BlindMI-w	Label-only	3	A > B	A < B	2+3+4	ES01:T100_N+0.530+0.038+2% ES21:T100_N+0.734+0.038+2%	CV2 40%	AR53	BlindMI-without	Top1_Threshold	3	A > B	A < B	6+7	ES23:CH_M_N+1.720+0.083+45% ES21:CH_M_N+1.720+0.083+20%	CV4 40%
AR12	Label-only	Top3_NN	3	A > B	A < B	1+2+3+5+6	ES07:C100_N+2.893+0.157+45% ES03:C100_N+2.893+0.085+45%	CV3 40%	AR54	Risk score	Top1_Threshold	-	A > B	A < B	3+6	ES20:P100_N+0.625+0.156+12% ES28:P100_N+0.729+0.156+12%	CV2 40%
AR13	BlindMI-without	Label-only	3	A > B	A < B	1+2+3	ES01:CH_M_N+0.954+0.083+20% ES21:CH_M_N+1.720+0.083+20%	CV2 40%	AR55	NN_attack	Top1_Threshold	3	A > B	A < B	6	ES21:P100_N+0.729+0.087+2% ES09:P100_N+0.625+0.104+4%	CV2 40%
AR14	Label-only	NN_attack	3	A > B	A < B	1+2+3+4+5+7	ES63:C100_B+2.893+0.157+45% ES59:C100_B+2.893+0.085+45%	CV3 40%	AR56	Top1_Threshold	Distillation-based	-	A > B	A < B	6	ES14:P100_N+0.625+0.110+4% ES16:P100_N+0.625+0.110+12%	CV4 40%
AR15	BlindMI-w	Top1_Threshold	3	A > B	A < B	1+2+5	ES35:C100_U+2.893+0.157+45% ES31:C100_U+2.893+0.085+45%	CV3 40%	AR57	Top1_Threshold	Shapley values	-	A > B	A < B	6	ES41:CH_M_U+1.355+0.108+49% ES44:CH_M_U+1.355+0.108+49%	CV4 40%
AR16	BlindMI-w	Top3_NN	3	A > B	A < B	1+2+3+4+6	ES07:C100_N+2.893+0.157+45% ES03:C100_N+2.893+0.085+45%	CV3 40%	AR58	Label-only	Shapley values	-	A > B	A < B	3+4+6+7	ES50:L30_U+0.801+0.041+8% ES78:L30_U+0.801+0.041+8%	CV1 40%
AR17	BlindMI-w	BlindMI-without	3	A > B	A < B	1+2+3+4+5	ES35:C100_U+2.893+0.157+45% ES31:C100_U+2.893+0.085+45%	CV3 40%	AR59	Calibrated Score	PPV	5	A > B	A < B	5+6+7	ES24:L30_N+0.801+0.076+8% ES04:L30_N+0.570+0.076+8%	CV2 40%
AR18	BlindMI-w	NN_attack	3	A > B	A < B	2+3+4	ES63:C100_B+2.893+0.157+45% ES59:C100_B+2.893+0.085+45%	CV3 40%	AR60	LiRA	Calibrated Score	1	A > B	A < B	5+6+7	ES27:L30_N+0.801+0.094+12% ES23:L30_N+0.801+0.041+12%	CV3 40%
AR19	BlindMI-without	Top3_NN	3	A > B	A < B	1+2+3+4	ES36:C100_U+2.893+0.157+49% ES34:C100_U+2.893+0.119+49%	CV3 40%	AR61	BlindMI-w	PPV	-	A > B	A < B	4+5+6+7	ES45:L30_U+0.724+0.094+4% ES37:L30_U+0.724+0.041+4%	CV3 40%
AR20	BlindMI-without	Calibrated Score	-	A > B	A < B	1+2+3	ES35:C100_U+2.893+0.157+45% ES31:C100_U+2.893+0.085+45%	CV3 40%	AR62	BlindMI-w	LiRA	-	A > B	A < B	4+5+6+7	ES74:P100_B+0.625+0.156+4% ES70:P100_B+0.625+0.110+4%	CV3 40%
AR21	BlindMI-without	NN_attack	3	A > B	A < B	1+2+3+4	ES01:C100_N+2.893+0.085+20% ES21:C100_N+4.325+0.085+20%	CV2 40%	AR63	BlindMI-ICLASS	PPV	-	A > B	A < B	1+4+6+7	ES20:L30_N+0.724+0.094+16% ES16:L30_N+0.724+0.076+16%	CV3 40%
AR22	Calibrated Score	NN_attack	1	A > B	A < B	1+2+3+4	ES11:C100_N+3.813+0.085+45% ES19:C100_N+3.813+0.157+45%	CV3 40%	AR64	BlindMI-ICLASS	LiRA	-	A > B	A < B	3+4+5+6	ES49:P100_U+0.729+0.087+2% ES29:P100_U+0.550+0.087+2%	CV2 40%
AR23	Calibrated Score	BlindMI-ICLASS	-	A > B	A < B	1+2+3+6+7	ES23:C100_N+4.325+0.085+45% ES03:C100_N+2.893+0.085+45%	CV2 40%	AR65	Top3_NN	PPV	-	A > B	A < B	4+6	ES15:P100_N+0.625+0.110+10% ES25:P100_N+0.729+0.110+10%	CV2 40%
AR24	LiRA	Distillation-based	1	A > B	A < B	1+2+3+4	ES01:C100_N+2.893+0.085+20% ES03:C100_N+2.893+0.085+45%	CV4 40%	AR66	Top3_NN	LiRA	-	A > B	A < B	4+6	ES40:ImaN_U+1.130+0.046+20% ES37:ImaN_U+1.130+0.046+20%	CV4 40%
AR25	Distillation-based	Shapley values	-	A > B	A < B	1+2+3+5+6	ES21:C100_N+4.325+0.085+20% ES01:C100_N+2.893+0.085+20%	CV2 40%	AR67	Shapley values	BlindMI-w	-	A > B	A < B	4	ES44:ImaN_U+1.130+0.080+49% ES41:ImaN_U+1.130+0.080+20%	CV4 40%
AR26	PPV	Distillation-based	1	A > B	A < B	1+2+3+4	ES01:C100_N+2.893+0.085+20% ES03:C100_N+2.893+0.085+20%	CV2 40%	AR68	Shapley values	NN_attack	-	A > B	A < B	3+4+5+7	ES56:CH_M_U+1.720+0.133+49% ES55:CH_M_U+1.720+0.133+45%	CV4 40%
AR27	LiRA	Shapley values	-	A > B	A < B	2+3+5	ES01:C100_N+2.893+0.085+20% ES03:C100_N+2.893+0.085+45%	CV4 40%	AR69	Shapley values	PPV	-	A > B	A < B	3+4	ES60:CH_M_B+0.954+0.108+40% ES80:CH_M_B+1.720+0.108+40%	CV2 40%
AR28	LiRA	PPV	1	A > B	A < B	1+2+3+4+5+6	ES77:C10_B+3.472+0.155+20% ES57:C10_B+1.908+0.155+20%	CV2 40%	AR70	Distillation-based	NN_attack	6	A > B	A < B	3+4+5+7	ES03:CH_M_N+0.954+0.083+45% ES07:CH_M_N+0.954+0.133+45%	CV3 40%
AR29	Top1_Threshold	Loss-Threshold	3	A > B	A < B	1+3+6	ES28:C100_N+3.472+0.291+49% ES26:C100_N+3.472+0.213+49%	CV3 40%	AR71	Distillation-based	BlindMI-ICLASS	-	A > B	A < B	3+4	ES23:ImaN_N+1.388+0.080+45% ES25:ImaN_N+1.388+0.080+45%	CV3 40%
AR30	BlindMI-w	Loss-Threshold	3	A > B	A < B	1+5	ES79:C100_B+3.472+0.155+45% ES09:C100_B+1.908+0.155+45%	CV2 40%	AR72	Distillation-based	BlindMI-without	-	A > B	A < B	3+4	ES29:ImaN_U+0.934+0.046+20% ES49:ImaN_U+1.388+0.046+20%	CV2 40%
AR31	Loss-Threshold	Top3_NN	3	A > B	A < B	1	ES17:C100_N+2.501+0.291+20% ES59:C100_B+1.908+0.155+45%	CV3 40%	AR73	LiRA	NN_attack	1	A > B	A < B	4	ES78:ImaN_B+1.130+0.046+40% ES66:ImaN_B+1.130+0.046+40%	CV2 40%
AR32	Top1_Threshold	BlindMI-ICLASS	3	A > B	A < B	1	ES59:C100_B+1.908+0.155+45% ES79:C100_B+3.472+0.155+45%	CV2 40%	AR74	PPV	NN_attack	7	A > B	A < B	4	ES37:L30_U+0.724+0.041+4% ES45:L30_U+0.724+0.094+4%	CV3 40%
AR33	Top3_NN	Top1_Threshold	4	A > B	A < B	1	ES38:P100_U+0.625+0.087+4% ES46:P100_U+0.625+0.156+4%	CV3 40%	AR75	LiRA	BlindMI-without	-	A > B	A < B	4+5	ES40:ImaN_U+1.130+0.046+49% ES48:ImaN_U+1.130+0.145+49%	CV3 40%
AR34	BlindMI-w	BlindMI-ICLASS	3	A > B	A < B	1+4+6+7	ES31:C100_U+1.908+0.155+45% ES35:C100_U+1.908+0.291+45%	CV3 40%	AR76	PPV	BlindMI-without	-	A > B	A < B	3+4+5	ES50:L30_U+0.801+0.041+8% ES30:L30_U+0.570+0.041+8%	CV2 40%
AR35	BlindMI-without	BlindMI-ICLASS	3	A > B	A < B	1	ES24:ImaN_N+1.388+0.080+40% ES04:ImaN_N+0.934+0.080+40%	CV2 40%	AR77	Top2+True	Distillation-based	1	A > B	A < B	3+5	ES21:T100_N+0.734+0.038+2% ES01:T100_N+0.530+0.038+2%	CV2 40%
AR36	Top2+True	Calibrated Score	-	A > B	A < B	1+3+4	ES07:C100_N+1.908+0.291+45% ES03:C100_N+1.908+0.155+45%	CV3 40%	AR78	Distillation-based	Label-only	-	A > B	A < B	3+5+7	ES39:L30_U+0.724+0.041+12% ES37:L30_U+0.724+0.041+4%	CV4 40%
AR37	BlindMI-ICLASS	Top2+True	3	A > B	A < B	1	ES35:C100_U+1.908+0.291+45% ES31:C100_U+1.908+0.155+45%	CV3 40%	AR79	Shapley values	BlindMI-ICLASS	-	A > B	A < B	3+5	ES33:L30_U+0.570+0.076+12% ES53:L30_U+0.801+0.076+12%	CV2 40%
AR38	BlindMI-ICLASS	NN_attack	-	A > B	A < B	1+3+4	ES50:C100_U+3.472+0.155+40% ES30:C100_U+1.908+0.155+40%	CV2 40%	AR80	LiRA	Loss-Threshold	1	A > B	A < B	5	ES22:L30_N+0.801+0.041+8% ES02:L30_N+0.570+0.041+8%	CV2 40%
AR39	Top3_NN	NN_attack	3+4	A > B	A < B	1+3+4+5+7	ES01:C100_N+1.908+0.155+20% ES57:C100_B+1.908+0.155+20%	CV1 40%	AR81	LiRA	Top1_Threshold	-	A > B	A < B	5	ES53:L30_U+0.801+0.076+12% ES43:L30_U+0.724+0.076+12%	CV2 40%
AR40	Calibrated Score	Label-only	-	A > B	A < B	1+3	ES01:C100_N+1.908+0.155+20% ES21:C100_N+3.472+0.155+20%	CV2 40%	AR82	Top1_Threshold	PPV	-	A > B	A < B	5	ES32:CH_M_U+0.954+0.108+40% ES34:CH_M_U+0.954+0.108+49%	CV4 40%
AR41	Calibrated Score	Top3_NN	-	A > B	A < B	1+3+6	ES74:C100_B+2.501+0.291+40% ES66:C100_B+2.501+0.155+40%	CV3 40%	AR83	BlindMI-without	Shapley values	-	A > B	A < B	3		
AR42	BlindMI-ICLASS	Label-only	-	A > B	A < B	1+3											

ARN.: the number of the attack ranking; EL.: Existing literature, where 1 → the LiRA attacks [55]; 2 → Risk score-based attacks [52]; 3 → BlindMI-Diff attacks [14]; 4 → the Top3-NN attacks [9]; 5 → the Calibrated Score-based attacks [56]; 6 → the Distillation-based Threshold attacks [53]; 7 → the PPV attacks [50]; - → the ranking of these two attacks does not existing in the existing literature; RAR.: replicate the attack ranking of the existing literature; dataset: 1 → CIFAR10 (C10); 2 → CIFAR100 (C100); 3 → CH_MNIST (CH_M); 4 → ImageNet (ImaN); 5 → Location30 (L30); 6 → Purchase100 (P100); 7 → Texas100 (T100); RES.: Evaluation Scenarios of replicated attacks (upper) and our experiments (lower); MR.: the main reason for the opposite rank of the attacks, where CV1 → the distance distribution of data samples in the target dataset, CV2 → the distance between data samples of the target dataset, CV3 → the differential distance between two datasets, CV4 → the ratio of the samples that are made no inferences by an MI attack; SMR.: the summary of the main reason for the opposite rank of the attacks, where CV1, CV2, CV3 and CV4 accounted for 2.41%, 40.96%, 37.35% and 19.28% respectively.

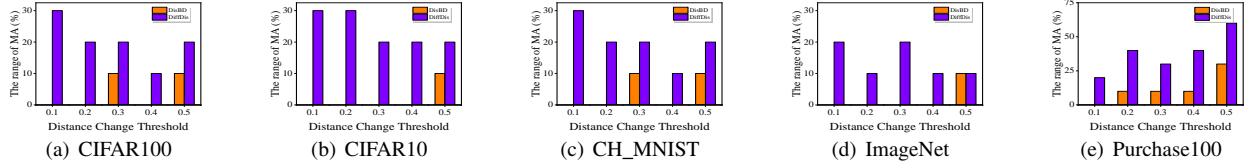


Figure 7. The comparisons of the effect of the distance between data samples of the target dataset (DisBD) and the differential difference between two datasets (DiffDis) on MA.

LiRA attacks combined per-example difficulty scores with a principled and well-calibrated Gaussian likelihood estimate, and they utilized a true-positive rate at low FPR metric to help determine the value of the threshold. Therefore, it hardly affects the ranking order of them when only the CV2 changes, which does not effect the prior distribution of the training data of the target model and does not effect the differences of the members and nonmembers; and changing only the CV4 will change the ratio of the samples of the target dataset, and the removed samples that are made no inferences by an MI attack may have high difficulty scores, this will increase the evaluation results of the LiRA attacks, and finally make the ranking order of the two attacks change. Moreover, from Figure 11, we find that the FNR is almost the same with the increase in sample distances.

[Observation] *The larger the distance between data samples of the target dataset, the higher the MA.*

[Observation] *The distance between data samples of the target dataset have little effect on the FNR.*

6.3. RQ3: Effect of Differential Distances between Two Datasets

Methodology. After constructing distance distributions of data samples and calculating the distance between data samples of the target dataset, we first generate a dataset with nonmembers via transforming existing samples into new samples or directly using the test data [14], and then we compute the differential distance between two datasets before and after a data sample with high output probability (a data sample with low output probability) (classified in Section 6.1) is moved from the target dataset to a nonmember dataset. And we get the average differential distance of data samples with high output probability and the average differential distance of data samples with low output probability between two datasets. Finally, we verify the evaluation results of 15 state-of-the-art MI attacks when only the differential distance between two datasets (e.g., the target dataset and the nonmember dataset) (CV3) is allowed to change and other three CVs (see Section 5.2.1) are left unchanged. Moreover, we design a distance interval threshold δ and compare the evaluation results when the distance between data samples of the target dataset and the differential distance between two datasets are changed to the same distance threshold (e.g., δ), respectively.

Results. From Figure 3 we find that the MA increases with the differential distance between two datasets (e.g., the target dataset and the nonmember dataset) increases.

[Observation] *The more the differential difference between two datasets, the higher the attacker-side MA.*

From Figure 7, we find that the effect of the distance between data samples of the target dataset on MA almost is 0, whereas that of the differential difference between two datasets is up to 30%, when the distance between data samples of the target dataset and the differential difference between two datasets are changed to the same distance threshold (e.g., 0.1). Moreover, from Table 8, we find that the change of average distances between data samples of the target dataset (e.g., 0.113) on CIFAR10 are larger than that of the average differential differences between two datasets (e.g., 0.082) when the MA is changed to the same threshold (e.g., 10%). From Figure 12, we find that the FNR is almost zero when the differential distance between two datasets changes.

[Observation] *The effect of the differential distance between two datasets on MA is larger than that of the distance between data samples of the target dataset.*

[Observation] *The differential distance between two datasets have little effect on the FNR.*

We observe that the ranking results of a particular MI attack (i.e. Label-only [13] (Class 2.1 see Figure 6)) remain **unchanged** across almost all the ESs in a particular group (i.e., when only the CV3 changed and other three CVs remained the same, the Label-only [13] is 70.88% of the top three to top seven most effective attacks). This indicates that the corresponding tuning variable probably does not affect the MI attack. To confirm this conclusion, we look into the algorithm of the MI attack and find the following: Label-only [13] mainly classified a sample as a member if the predicted class was the same as its ground-truth label. Therefore, when only the CV3 changes and other three CVs remain the same, it does not affect the ground-truth labels of the target dataset, and thus has little effect on the Label-only [13] attack.

We find that the BlindMI-Diff-w [14] (Class 3.1.1 see Figure 6) is most affected when only the CV3 changes, other three CVs remain the same, for example, for one particular evaluation scenario ES03 on ImageNet could result in the following ranking: Class 2.1 (except for the Label-only and Top1_Threshold attacks) > Class 2.2.1 > Class 3.1.1 > Class 1.1.1 (except for the NN attack) > Class 2.2.2 (except for the Calibrated Score, LiRA, PPV attacks) > Class 3.1.3 > Class

3.1.2 > Class 1.1.2, and for another particular evaluation scenario ES05 on ImageNet could result in the following ranking: Class 2.1 (except for the Label-only and Top1_Threshold attacks) > Class 2.2.1 > Class 1.1.1 (except for the Top3 NN attack) > Class 2.2.2 (except for the Calibrated Score, LiRA attack) > Class 3.1.3 > Class 3.1.2 > Class 3.1.1 > Class 1.1.2. The reason is that the BlindMI-Diff-w attack [14] mainly utilized the differences between two datasets before and after a sample was moved, and when only the CV3 changes, the differential distance between two datasets will change, which will affect evaluation results.

We also observe that the ranking order between two particular MI attacks (i.e. Label-only (Class 2.1 see Figure 6) and NN_attack (Class 1.1.1 see Figure 6)) remain **unchanged** across almost all the ESs in a particular group. This indicates that the ranking order is independent of the control variable. In addition, this indicates that the ranking order is to certain extent determined by the three non-tuning factors. We look into the values of the three non-tuning factors, and we find that the ranking order between Label-only and NN_attacks is NN_attack > Label-only when only the CV3 changes and other three CVs remain the same, while the ranking order of them is Label-only > NN_attack when only the CV1 changes and other three variables remain the same. The reason is that it hardly affects the ranking order of them when only the CV3 changes, which does not effect the ground-truth labels and output probabilities of the target dataset; and changing only the CV1 may cause NN_attacks to be unable to effectively distinguish between members and nonmembers of different distance distributions of data samples in the target dataset, and finally make the ranking order of the two attacks change.

6.4. RQ4: Effect of the Ratios of the samples that are made no inferences by an MI attack

Methodology. For each distance distribution of data samples, the distance between data samples and the differential distance between two datasets of the target dataset, we first set different ratios of the samples that are made no inferences by an MI attack for image (e.g., 20%, 40%, 45% and 49%) and text datasets (e.g., 2%, 4%, 10% and 12%) as the prior Privacy Risk Scores-based [52] and the Shapley Values-based MI attacks [54]. Then, we verify the evaluation results of 15 state-of-the-art MI attacks when only the ratio of the samples that are made no inferences by an MI attack (CV4) is allowed to change and other three CVs (see Section 5.2.1) are left unchanged.

Results. From Figure 5, we find that the evaluations are different when the ratios are different. We observe that the ranking results of a particular MI attack (i.e. NN_attack [8] (Class 1.1.1 see Figure 6)) remain **unchanged** across almost all the ESs in a particular group (i.e., when only the CV4 changed and other three CVs remained the same, the NN_attack [8] is 88.95% of the top five to top nine most effective attacks). This indicates that the corresponding tuning variable probably does not affect the MI attack.

To confirm this conclusion, we look into the algorithm of the MI attack and find the following: NN_attack [8] was mainly based on the output probability of the target model. Therefore, when only the CV4 changes and other three CVs remain the same, it does not affect the output probability of data samples in the target dataset, and thus has little effect on the NN_attack [8].

We find that the Shapley Values [54] attack (Class 2.2.1 see Figure 6) is most affected when only the CV4 changes, other three CVs remain the same, for example, for one particular ES49 on ImageNet could result in the following ranking: Class 2.1 (except for the Label-only and Top1_Threshold) > Class 3.1.1 > Class 1.1.1 (except for the Top3_NN attack) > Class 2.2.1 (except for the Risk score attack) > Class 2.2.2 (except for the LiRA, Calibrated Score attacks) > Class 3.1.3 > Class 3.1.2 > Class 1.1.2, and for another particular ES50 on ImageNet could result in the following ranking: Class 2.1 (except for the Label-only and Top1_Threshold attacks) > Class 2.2.1 > Class 1.1.1 (except for the NN attack) > Class 2.2.2 (except for the PPV, Calibrated Score attacks) > Class 3.1.3 > Class 3.1.2 > Class 3.1.1 > Class 1.1.2. The reason is that the Shapley Values [54] attack mainly set meaningful thresholds for SHAPr scores to decide whether a data record is susceptible to MI attacks, and when only the CV4 changes, the Shapley Values [54] attack will select the data samples that have high shapley values to infer their membership, which will affect evaluation results.

We observe that the ranking results of a particular MI attack (i.e. BlindMI-Diff-w [14] (Class 3.1.1 see Figure 6)) remain unchanged across almost all the ESs in Group A (e.g., ES49: C100_U+4.325+0.085+20%, ES50: C100_U + 4.325+0.085+40% and ES51: C100_U + 4.325+0.085+45%). We also observe that the ranking results of the same MI attack remain unchanged across almost all the ESs in Group B (e.g., ES55: C100_U+ 4.325+0.157+45%, ES56: C100_U+4.325+0.157+49%). Note that Group A and Group B use the same tuning variable such as the CV4. However, the ranking results are different between the two groups. This indicates that the MI attack is probably affected by the differences between the values of the three non-tuning factors in the two groups. We look into the differences and find that the differences between the values of the three non-tuning factors in the two groups are the CV3 (e.g., 0.085 and 0.157) and BlindMI-Diff-w [14] mainly utilized the differences between two datasets before and after a sample was moved. Therefore, the BlindMI-Diff-w attacks are most affected by the CV3.

We also observe that the ranking results of the Shapley Values [54] attack (Class 2.2.1 see Figure 6) remain unchanged across almost all the ESs in Group A (e.g., ES31: C100_U+2.893+0.085+45%, ES33: C100_U + 2.893 + 0.119+45% and ES35: C100_U+2.893+0.157+45%) and Group B (e.g., ES34: C100_U+2.893+0.119+49%, ES36: C100_U+2.893+0.157+49%). Note that Group A and Group B use the same tuning variable such as the CV3. However, the ranking results are different between the two groups (e.g., the second and the third). We look into the

differences and find that the differences between the values of the three non-tuning factors in the two groups are the CV4 (e.g., 45% and 49%) and Shapley Values attacks set meaningful thresholds for SHAPr scores to decide distinguish members, and when only CV4 changes, the Shapley Values attack will select the data samples that have high shapley values to infer their membership. Therefore, the Shapley Values attacks are most affected by the CV4.

7. Related Work

Membership Inference Attacks. Homer *et al.* [59] first proposed an MI attack on biological data. Shokri *et al.* [8] proposed the first black-box MI attack against ML. Huge literature followed these works to different scenarios (e.g., location data [60], language models [10], sentence embeddings [61], speech recognition models [62], federated learning [7], transfer learning [63], generative models [38], white box access [12], [21], [48]).

Categories of Membership Inference Attacks. There are main three categories **1) Binary classifier-based MI attacks**, which utilize the output predictions of shadow models to train a binary classifier to launch the MI attacks [8], [9]. **2) Evaluation metric-based MI attacks**, which used the defined evaluation metrics to distinguish members and nonmembers [9], [13], [14], [37], [39], [51]. **3) Differential Comparisons-based MI attacks (BlindMI-Diff)**, which mainly utilized the differences between two datasets.

Defenses against MI attacks. Multiple defenses [8], [9], [11], [64], [65], [66], [67], [68] have been proposed to mitigate MI attacks.

8. Conclusion

In this paper, we seek to develop a comprehensive benchmark for comparing different MI attacks. The primary design goal of our benchmark, called **MIBench**, is to meet *all* of above-mentioned 4 requirements (see Section 1). Our benchmark consists not only the evaluation metrics, but also the evaluation scenarios. And we design the evaluation scenarios from **four perspectives**: the distance distribution of data samples in the target dataset, the distance between data samples of the target dataset, the differential distance between two datasets (i.e., the target dataset and a generated dataset with only nonmembers), and the ratio of the samples that are made no inferences by an MI attack. The evaluation metrics consist of ten typical evaluation metrics. We have identified three principles for the proposed “comparing different MI attacks” methodology, and we have designed and implemented the MIBench benchmark with 84 evaluation scenarios for each dataset. In total, we have used our benchmark to fairly and systematically compare 15 state-of-the-art MI attack algorithms across 588 evaluation scenarios, and these evaluation scenarios cover 7 widely used datasets and 7 representative types of models.

References

- [1] K. He, X. Zhang, S. Ren, and J. Sun, “Deep residual learning for image recognition,” in *CVPR*, 2016.
- [2] A. Hannun, C. Case, J. Casper, B. Catanzaro, G. Diamos, E. Elsen, R. Prenger, S. Sathesh, S. Sengupta, A. Coates *et al.*, “Deep speech: Scaling up end-to-end speech recognition,” *arXiv preprint arXiv:1412.5567*, 2014.
- [3] J. Devlin, M.-W. Chang, K. Lee, and K. Toutanova, “Bert: Pre-training of deep bidirectional transformers for language understanding,” *arXiv preprint arXiv:1810.04805*, 2018.
- [4] E. Choi, M. T. Bahadori, A. Schuetz, W. F. Stewart, and J. Sun, “Doctor ai: Predicting clinical events via recurrent neural networks,” in *PMLR*, 2016.
- [5] C. Song and V. Shmatikov, “Overlearning reveals sensitive attributes,” in *ICLR*, 2020.
- [6] I. Rosenberg, A. Shabtai, Y. Elovici, and L. Rokach, “Adversarial machine learning attacks and defense methods in the cyber security domain,” *CSUR*, 2021.
- [7] M. S. Jere, T. Farnan, and F. Koushanfar, “A taxonomy of attacks on federated learning,” *SP*, 2020.
- [8] R. Shokri, M. Stronati, C. Song, and V. Shmatikov, “Membership inference attacks against machine learning models,” in *SP*, 2017.
- [9] A. Salem, Y. Zhang, M. Humbert, M. Fritz, and M. Backes, “MI-leaks: Model and data independent membership inference attacks and defenses on machine learning models,” in *NDSS*, 2019.
- [10] N. Carlini, F. Tramer, E. Wallace, M. Jagielski, A. Herbert-Voss, K. Lee, A. Roberts, T. Brown, D. Song, U. Erlingsson *et al.*, “Extracting training data from large language models,” in *USENIX Security*, 2021.
- [11] J. Jia, A. Salem, M. Backes, Y. Zhang, and N. Z. Gong, “Memguard: Defending against black-box membership inference attacks via adversarial examples,” in *CCS*, 2019.
- [12] A. Sablayrolles, M. Douze, C. Schmid, Y. Ollivier, and H. Jégou, “White-box vs black-box: Bayes optimal strategies for membership inference,” in *ICML*, 2019.
- [13] S. Yeom, I. Giacomelli, M. Fredrikson, and S. Jha, “Privacy risk in machine learning: Analyzing the connection to overfitting,” in *CSF*, 2018.
- [14] B. Hui, Y. Yang, H. Yuan, P. Burlina, N. Z. Gong, and Y. Cao, “Practical blind membership inference attack via differential comparisons,” in *NDSS*, 2021.
- [15] C. Song and R. Shokri, “Robust membership encoding: Inference attacks and copyright protection for deep learning,” *arXiv e-prints*, 2019.
- [16] Y. Liu, R. Wen, X. He, A. Salem, Z. Zhang, M. Backes, E. De Cristofaro, M. Fritz, and Y. Zhang, “MI-doctor: Holistic risk assessment of inference attacks against machine learning models,” in *USENIX Security*, 2022.
- [17] S. Hisamoto, M. Post, and K. Duh, “Membership inference attacks on sequence-to-sequence models: Is my data in your machine translation system?” *ACL*, 2020.
- [18] S. P. Liew and T. Takahashi, “Faceleaks: Inference attacks against transfer learning models via black-box queries,” *arXiv preprint arXiv:2010.14023*, 2020.
- [19] M. Chen, Z. Zhang, T. Wang, M. Backes, M. Humbert, and Y. Zhang, “When machine unlearning jeopardizes privacy,” in *CCS*, 2021.
- [20] Y. He, S. Rahimian, B. Schiele, and M. Fritz, “Segmentations-leak: Membership inference attacks and defenses in semantic image segmentation,” in *ECCV*, 2020.
- [21] M. Nasr, R. Shokri, and A. Houmansadr, “Comprehensive privacy analysis of deep learning: Passive and active white-box inference attacks against centralized and federated learning,” in *SP*, 2019.

- [22] H. Ha, J. Jang, Y. Jeong, and S. Yoon, "Membership feature disentanglement network," in *CCS*, 2022.
- [23] Y. Gu, Y. Bai, and S. Xu, "Cs-mia: Membership inference attack based on prediction confidence series in federated learning," *Journal of Information Security and Applications*, 2022.
- [24] H. Liu, J. Jia, W. Qu, and N. Z. Gong, "Encodermi: Membership inference against pre-trained encoders in contrastive learning," in *CCS*, 2021.
- [25] R. Webster, J. Rabin, L. Simon, and F. Jurie, "This person (probably) exists. identity membership attacks against gan generated faces," *arXiv preprint arXiv:2107.06018*, 2021.
- [26] G. Li, S. Rezaei, and X. Liu, "User-level membership inference attack against metric embedding learning," *arXiv preprint arXiv:2203.02077*, 2022.
- [27] Y. Yang, P. Gohari, and U. Topcu, "On the vulnerability of recurrent neural networks to membership inference attacks," *arXiv preprint arXiv:2110.03054*, 2021.
- [28] M. Zhang, Z. Ren, Z. Wang, P. Ren, Z. Chen, P. Hu, and Y. Zhang, "Membership inference attacks against recommender systems," in *CCS*, 2021.
- [29] Z. Zhang, M. Chen, M. Backes, Y. Shen, and Y. Zhang, "Inference attacks against graph neural networks," in *USENIX Security*, 2022.
- [30] C. Song, T. Ristenpart, and V. Shmatikov, "Machine learning models that remember too much," in *CCS*, 2017.
- [31] J. Li, N. Li, and B. Ribeiro, "Membership inference attacks and defenses in supervised learning via generalization gap," 2020.
- [32] F. Farokhi and M. A. Kaafar, "Modelling and quantifying membership information leakage in machine learning," *arXiv preprint arXiv:2001.10648*, 2020.
- [33] H. Chang and R. Shokri, "On the privacy risks of algorithmic fairness," in *SP*, 2021.
- [34] Y. Kaya, S. Hong, and T. Dumitras, "On the effectiveness of regularization against membership inference attacks," *arXiv preprint arXiv:2006.05336*, 2020.
- [35] N. Carlini, C. Liu, J. Kos, Ú. Erlingsson, and D. Song, "The secret sharer: Measuring unintended neural network memorization & extracting secrets," *arXiv preprint arXiv:1802.08232*, 2018.
- [36] A. Salem, A. Bhattacharya, M. Backes, M. Fritz, and Y. Zhang, "{Updates-Leak}: Data set inference and reconstruction attacks in online learning," in *USENIX Security*, 2020.
- [37] C. A. Choquette-Choo, F. Tramer, N. Carlini, and N. Papernot, "Label-only membership inference attacks," in *ICML*, 2021.
- [38] D. Chen, N. Yu, Y. Zhang, and M. Fritz, "Gan-leaks: A taxonomy of membership inference attacks against generative models," in *CCS*, 2020.
- [39] Z. Li and Y. Zhang, "Membership leakage in label-only exposures," in *CCS*, 2021.
- [40] J. Chen, J. Zhang, Y. Zhao, H. Han, K. Zhu, and B. Chen, "Beyond model-level membership privacy leakage: an adversarial approach in federated learning," in *ICCCN*, 2020.
- [41] Z. Zhang, L. Y. Zhang, X. Zheng, B. H. Abbasi, and S. Hu, "Evaluating membership inference through adversarial robustness," *arXiv preprint arXiv:2205.06986*, 2022.
- [42] G. Del Grosso, H. Jalalzai, G. Pichler, C. Palamidessi, and P. Piantanida, "Leveraging adversarial examples to quantify membership information leakage," in *CVPR*, 2022.
- [43] S. Mahloujifar, A. Sablayrolles, G. Cormode, and S. Jha, "Optimal membership inference bounds for adaptive composition of sampled gaussian mechanisms," *arXiv preprint arXiv:2204.06106*, 2022.
- [44] D. Zhong, H. Sun, J. Xu, N. Gong, and W. H. Wang, "Understanding disparate effects of membership inference attacks and their countermeasures," in *CCS*, 2022.
- [45] S. Li, Y. Wang, Y. Li, and Y.-a. Tan, "l-leaks: Membership inference attacks with logits," *arXiv preprint arXiv:2205.06469*, 2022.
- [46] X. He and Y. Zhang, "Quantifying and mitigating privacy risks of contrastive learning," in *CCS*, 2021.
- [47] J. W. Bentley, D. Gibney, G. Hoppenworth, and S. K. Jha, "Quantifying membership inference vulnerability via generalization gap and other model metrics," *arXiv preprint arXiv:2009.05669*, 2020.
- [48] K. Leino and M. Fredrikson, "Stolen memories: Leveraging model memorization for calibrated {White-Box} membership inference," in *USENIX Security*, 2020.
- [49] S. Rezaei and X. Liu, "On the difficulty of membership inference attacks," in *CVPR*, 2021.
- [50] B. Jayaraman, L. Wang, K. Knipmeyer, Q. Gu, and D. Evans, "Revisiting membership inference under realistic assumptions," *arXiv preprint arXiv:2005.10881*, 2020.
- [51] Y. Long, L. Wang, D. Bu, V. Bindschaedler, X. Wang, H. Tang, C. A. Gunter, and K. Chen, "A pragmatic approach to membership inferences on machine learning models," in *SP*, 2020.
- [52] L. Song and P. Mittal, "Systematic evaluation of privacy risks of machine learning models," in *USENIX Security*, 2021.
- [53] J. Ye, A. Maddi, S. K. Murakonda, and R. Shokri, "Enhanced membership inference attacks against machine learning models," *arXiv preprint arXiv:2111.09679*, 2021.
- [54] V. Duddu, S. Szyller, and N. Asokan, "Shapr: An efficient and versatile membership privacy risk metric for machine learning," *arXiv preprint arXiv:2112.02230*, 2021.
- [55] N. Carlini, S. Chien, M. Nasr, S. Song, A. Terzis, and F. Tramer, "Membership inference attacks from first principles," in *SP*, 2022.
- [56] L. Watson, C. Guo, G. Cormode, and A. Sablayrolles, "On the importance of difficulty calibration in membership inference attacks," *arXiv preprint arXiv:2111.08440*, 2021.
- [57] A. Gretton, K. M. Borgwardt, M. J. Rasch, B. Schölkopf, and A. Smola, "A kernel two-sample test," *JMLR*, 2012.
- [58] K. M. Borgwardt, A. Gretton, M. J. Rasch, H.-P. Kriegel, B. Schölkopf, and A. J. Smola, "Integrating structured biological data by kernel maximum mean discrepancy," *Bioinformatics*, 2006.
- [59] N. Homer, S. Szelinger, M. Redman, D. Duggan, W. Tembe, J. Muehling, J. V. Pearson, D. A. Stephan, S. F. Nelson, and D. W. Craig, "Resolving individuals contributing trace amounts of dna to highly complex mixtures using high-density snp genotyping microarrays," *PLoS genetics*, 2008.
- [60] A. Pyrgelis, C. Troncoso, and E. De Cristofaro, "Measuring membership privacy on aggregate location time-series," *ACM MACS*, 2020.
- [61] C. Song and A. Raghunathan, "Information leakage in embedding models," in *CCS*, 2020.
- [62] M. A. Shah, J. Szurley, M. Mueller, A. Mouchtaris, and J. Droppo, "Evaluating the vulnerability of end-to-end automatic speech recognition models to membership inference attacks," in *Proc. Interspeech*, 2021.
- [63] Y. Zou, Z. Zhang, M. Backes, and Y. Zhang, "Privacy analysis of deep learning in the wild: Membership inference attacks against transfer learning," *arXiv preprint arXiv:2009.04872*, 2020.
- [64] M. Abadi, A. Chu, I. Goodfellow, H. B. McMahan, I. Mironov, K. Talwar, and L. Zhang, "Deep learning with differential privacy," in *CCS*, 2016.
- [65] M. Nasr, R. Shokri, and A. Houmansadr, "Machine learning with membership privacy using adversarial regularization," in *CCS*, 2018.
- [66] N. Srivastava, G. Hinton, A. Krizhevsky, I. Sutskever, and R. Salakhutdinov, "Dropout: a simple way to prevent neural networks from overfitting," *JMLR*, 2014.
- [67] V. Shejwalkar and A. Houmansadr, "Membership privacy for machine learning models through knowledge transfer," in *AAAI*, 2021.
- [68] J. Zheng, Y. Cao, and H. Wang, "Resisting membership inference attacks through knowledge distillation," *Neurocomputing*, 2021.

Appendix

A. Datasets Description

CIFAR100. CIFAR100 is a widely used benchmark dataset to image classification, which consists of 60,000 images in 100 classes. We randomly select two disjoint sets of 10,000 images as the target models and the shadow models' training datasets, respectively.

CIFAR10. CIFAR10 is a widely used dataset to evaluate the image classification, which consists of 60,000 images in 10 classes. We randomly select two disjoint sets of 10,000 images as the target models and the shadow models' training datasets, respectively.

CH_MNIST. CH_MNIST is a benchmark dataset of histological images used to evaluate human colorectal cancer, consisting of 5,000 histological images in 8 classes of tissues. We follow the same image processing methods and classification tasks as prior BlindMI-DIFF [14] to resize all images to 64×64 . We randomly select two disjoint sets of 2,500 images as the target models and the shadow models' training datasets, respectively.

ImageNet. Tiny-imagenet is a widely used benchmark dataset to image classification, which is a subset of the ImageNet dataset and consists of 100,000 images in 200 classes. We randomly select two disjoint sets of 10,000 images as the target models and the shadow models' training datasets, respectively.

Location30. Location30 contains location "check-in" records of individuals. We obtain a pre-processed dataset from [8] which contains 5,010 data samples with 446 binary features corresponding to whether an individual has visited a particular location. All data samples are clustered into 30 classes representing different geosocial types. The classification task is to predict the geosocial type based on the 466 binary features. Following *Jia et al.* [11], we use 1,000 data samples to train a target model.

Purchase100. Purchase100 contains shopping records of different individuals. We obtain a pre-processed dataset from [8] containing 197,324 data samples with 600 binary features corresponding to a specific product. All data samples are clustered into 100 classes representing different purchase styles. The classification task is to predict the purchase style based on the 600 binary features. We follow *Nasr et al.* [21], [65] to use 10% data samples (19,732) to train a target model.

Texas100. Texas100 consists of Texas Department of State Health Services' information about patients discharged from public hospitals. Each data record contains information about the injury, diagnosis, the procedures the patient underwent and some demographic details. We obtain preprocessed dataset from [8] which contains 100 classes of patient's procedures consisting 67,330 data samples with 6,170 binary features. The classification task is to predict the patient's main procedure based on the patient's information. Following [11], [21], [65], we use 10,000 data samples to train a target model.

B. Original and Constructed Distance Distributions of Data Samples in the Target Dataset

Figure 13 and Figure 14 show the original and constructed distance distribution of data samples in the target target seven datasets, respectively.

C. The Selected Distances of the Target Dataset

Table 9 shows the selected distances between data samples (*Dis_Between_Data*) and differential distances between two datasets of the target dataset in our experiments.

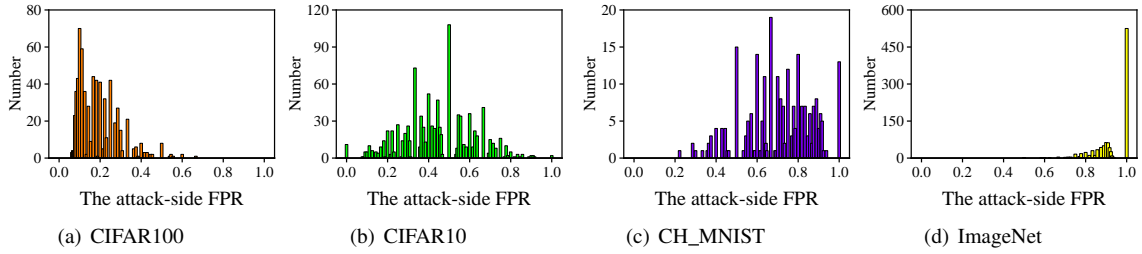


Figure 8. The distribution of the FPR of the BlindMI-Diff-w/ [14].

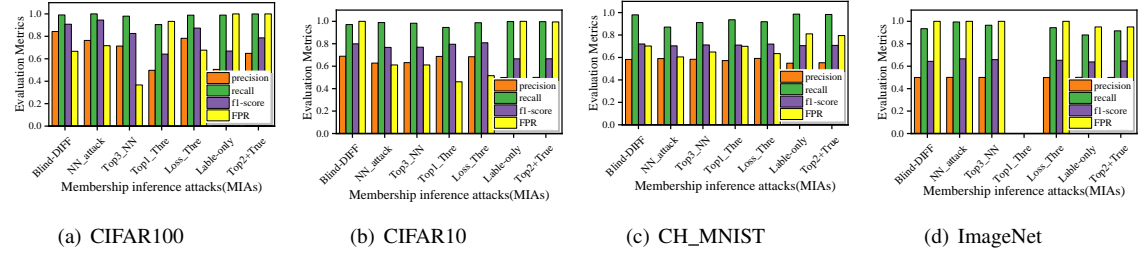


Figure 9. The evaluation of the existing MI attacks (e.g., the attacker-side precision, recall, f1-score and FPR).

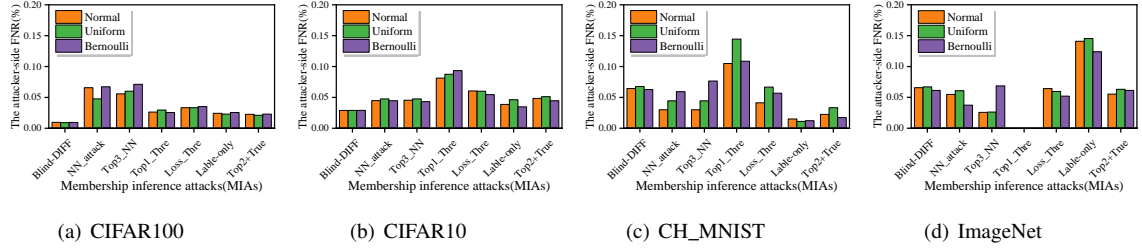


Figure 10. The attacker-side FNR of the distance distribution of the target datasets obeying normal, uniform and bernoulli distributions.

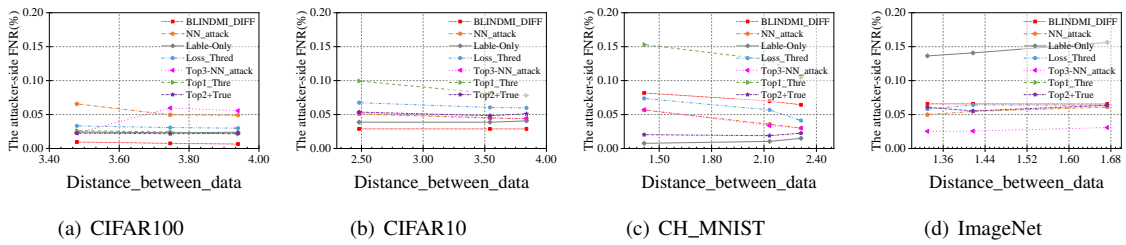


Figure 11. The effect of the distance between data samples of the target dataset on the attacker-side FNR.

TABLE 7. THE EFFECT OF THE DISTANCE BETWEEN DATA SAMPLES OF THE TARGET DATASET (DISDATA) ON THE ATTACKER-SIDE MEMBERSHIP ADVANTAGE.

Dataset	DisData	Attacker-side Membership Advantage (MA)								
		BlindMI-Diff	NN_attack	Label-only	Loss-Thres	Top3-NN	Top2+True	PPV	Calibrated Score	Distillation-based Thre
CIFAR100	3.823	61.63%	56.13%	75.38%	73.37%	60.25%	69.25%	1.83%	35.60%	25.86%
CIFAR10	2.573	53.34%	38.50%	33.50%	50.50%	38.38%	46.13%	-0.07%	33.61%	24.56%
CH_MNIST	1.315	27.72%	26.60%	17.60%	20.13%	26.24%	18.84%	-0.92%	22.04%	23.45%
ImageNet	1.138	0.47%	0.15%	0.56%	0.05%	0.08%	0.09%	-1.08%	-0.07%	23.12%

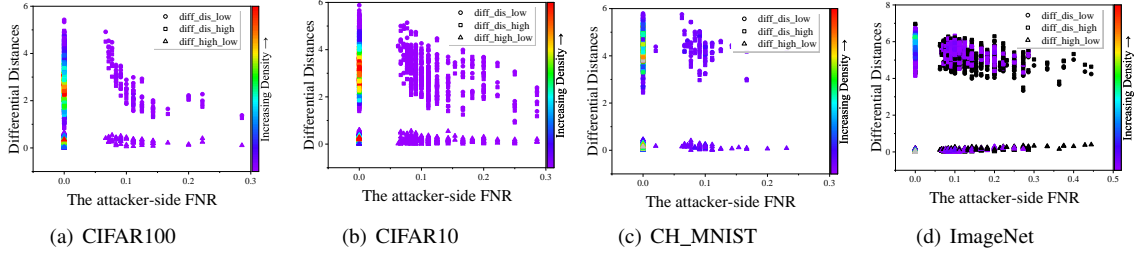


Figure 12. The effect of the differential distance between two datasets on attacker-side FNR.

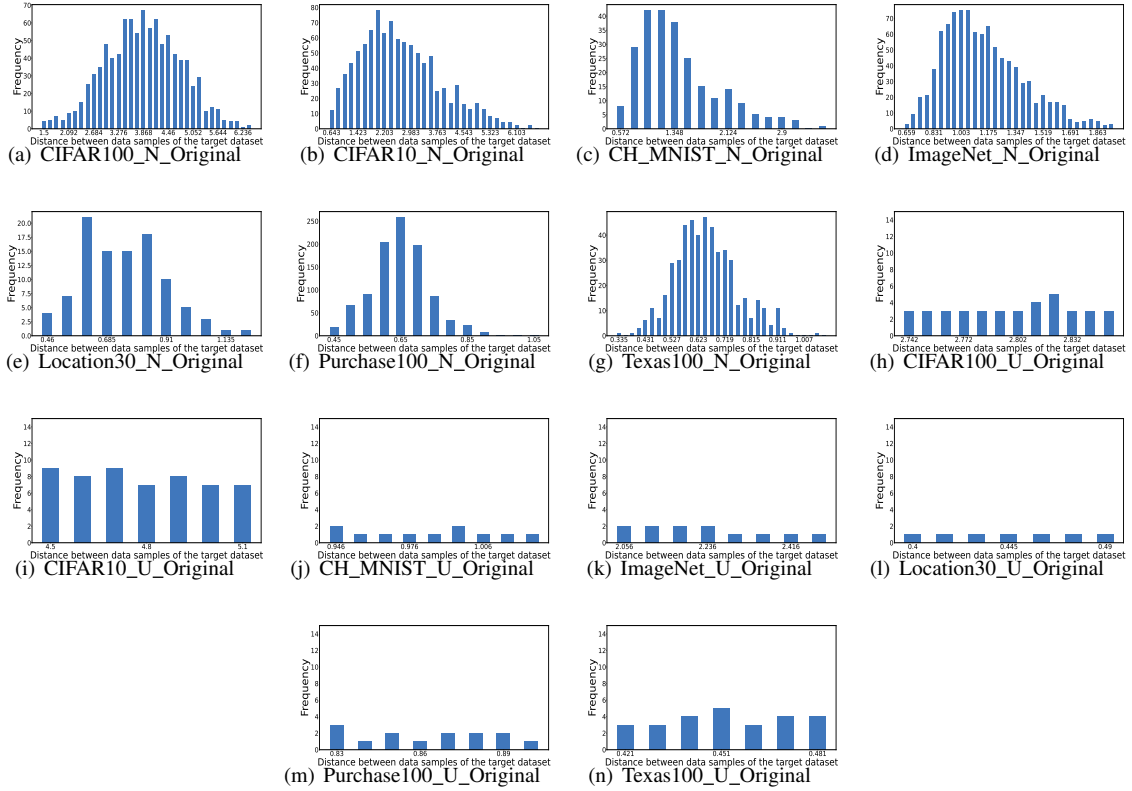


Figure 13. The Original Distance Distribution of Data Samples in the Target Dataset. Inside (a)-(g) are the original distance distributions of data samples in the target CIFAR100, CIFAR10, CH_MNIST, ImageNet, Location30, Purchase100 and Texas100 datasets approximately obey normal distributions, and (h)-(n) are the original distance distributions of data samples in the target seven datasets approximately obey uniform distributions.

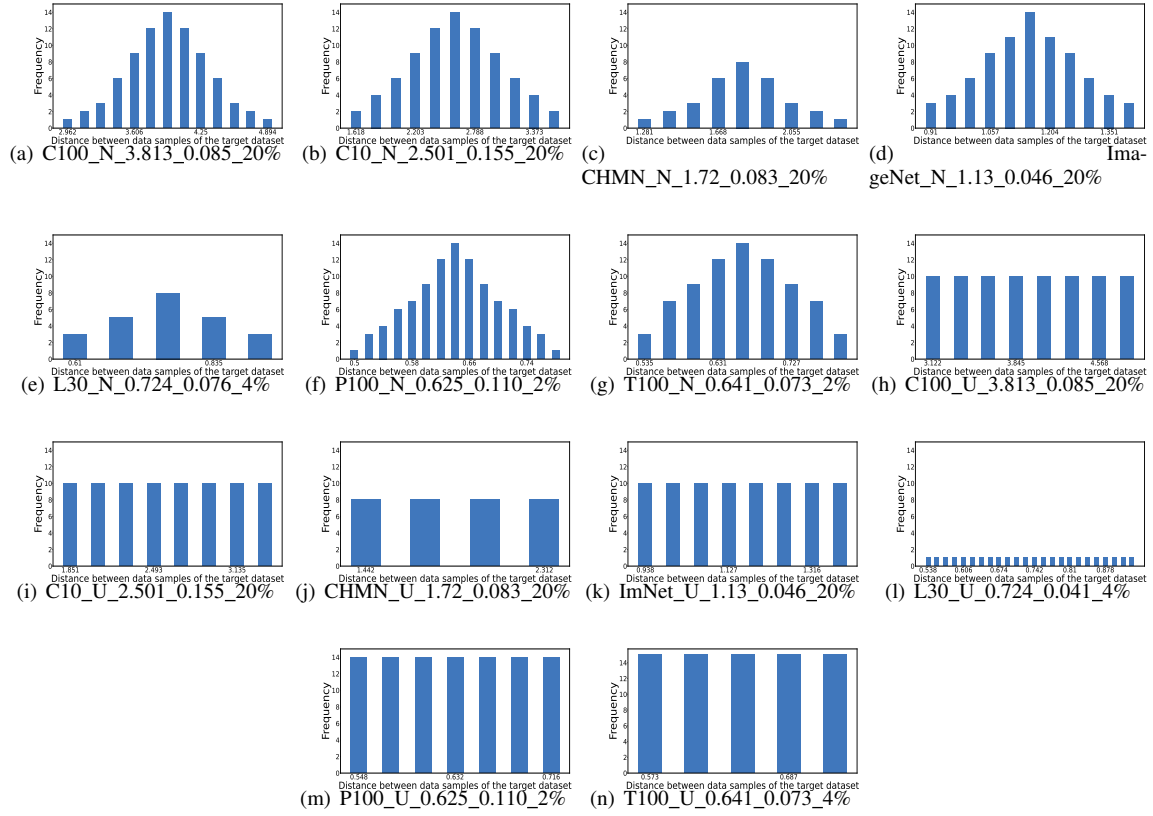


Figure 14. The Constructed Distance Distribution of Data Samples in the Target Dataset obeys Normal and Uniform Distribution, respectively. Inside (a)-(g) are the constructed distance distributions of data samples in the target CIFAR100 (C100), CIFAR10 (C10), CH_MNIST (CHMN), ImageNet, Location30 (L30), Purchase100 (P100) and Texas100 (T100) datasets obey normal distributions, and (h)-(n) are the constructed distance distributions of data samples in the target seven datasets obey uniform distributions.

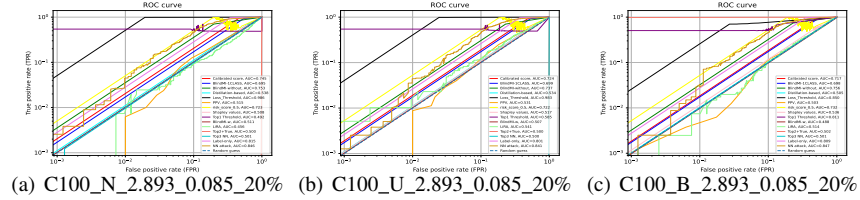


Figure 15. Comparing the true positive rate vs. false positive rate of prior 15 state-of-the-art membership inference attacks on CIFAR100 by the AUC computed as the Area Under the Curve of attack ROC in logarithmic scale. Inside (a)-(c) are the ROCs in logarithmic scale of the constructed distance distributions of data samples in the target CIFAR100 (C100) dataset obey normal, uniform and bernoulli distributions, respectively.

TABLE 8. THE AVERAGE DISTANCE BETWEEN DATA SAMPLES (DisBD) AND THE DIFFERENTIAL DISTANCE BETWEEN TWO DATASETS (DiffDis) CHANGE ON THE MA (C_MA).

Dataset	C_MA	average DisBD	average DiffDis
CIFAR100	10%	0.143	0.107
	20%	0.230	0.099
	30%	0.349	0.138
	40%	0.460	0.143
	50%	0.630	0.257
CIFAR10	10%	0.113	0.082
	20%	0.179	0.115
	30%	0.299	0.182
	40%	0.440	0.238
	50%	0.544	0.320
	60%	0.659	0.389
	70%	0.793	0.545
CH_MNIST	10%	0.140	0.091
	20%	0.249	0.158
	30%	0.335	0.237
	40%	0.476	0.328
	50%	0.638	0.408
	60%	0.843	0.547
ImageNet	10%	0.268	0.225
	20%	0.580	0.288
	30%	0.805	0.379

TABLE 9. THE SELECTED DISTANCES BETWEEN DATA SAMPLES (Dis_Between_Data) AND DIFFERENTIAL DISTANCES BETWEEN TWO DATASETS OF THE TARGET DATASET.

Dataset	Dis_Between_Data	Differential Distances
CIFAR100	2.893	0.085
	3.813	0.119
	4.325	0.157
CIFAR10	1.908	0.155
	2.501	0.213
	3.472	0.291
CH_MNIST	0.954	0.083
	1.355	0.108
	1.720	0.133
ImageNet	0.934	0.046
	1.130	0.080
	1.388	0.145
Location30	0.570	0.041
	0.724	0.076
	0.801	0.094
Purchase100	0.550	0.087
	0.625	0.110
	0.729	0.156
Texas1000	0.530	0.038
	0.641	0.073
	0.734	0.107

TABLE 10. THE PARAMETER (p) AND THRESHOLDS OF THE BERNOULLI DISTRIBUTION OF DATA SAMPLES IN THE TARGET DATASET.

Parameter (p)	Thresholds of Bernoulli Distribution in Different Datasets						
	C_100	C_10	CH	Image	L_30	P_100	T_100
0.1	2.623	1.147	0.729	0.835	0.520	0.504	0.512
0.2	2.97	1.529	0.837	0.906	0.574	0.554	0.551
0.3	3.306	1.84	0.935	0.964	0.608	0.566	0.578
0.4	3.535	2.097	1.081	1.021	0.660	0.608	0.605
0.5	3.778	2.39	1.186	1.081	0.705	0.620	0.630
0.6	4.013	2.707	1.30	1.153	0.750	0.635	0.661
0.7	4.259	3.064	1.45	1.227	0.784	0.675	0.692
0.8	4.555	3.513	1.765	1.323	0.845	0.688	0.729
0.9	4.913	4.285	2.19	1.491	0.920	0.741	0.813